

NASA/CR-1999-209729
ICASE Report No. 99-46



Minimization of the Truncation Error by Grid Adaptation

*Nail K. Yamaleev
NASA Langley Research Center, Hampton, Virginia*

*Institute for Computer Applications in Science and Engineering
NASA Langley Research Center
Hampton, VA*

Operated by Universities Space Research Association



National Aeronautics and
Space Administration

Langley Research Center
Hampton, Virginia 23681-2199

Prepared for Langley Research Center
under Contract NAS1-97046

November 1999

MINIMIZATION OF THE TRUNCATION ERROR BY GRID ADAPTATION

NAIL K. YAMALEEV*

Abstract. A new grid adaptation strategy, which minimizes the truncation error of a p th-order finite difference approximation, is proposed. The main idea of the method is based on the observation that the global truncation error associated with discretization on nonuniform meshes can be minimized if the interior grid points are redistributed in an optimal sequence. The method does not explicitly require the truncation error estimate and at the same time, it allows one to increase the design order of approximation by one globally, so that the same finite difference operator reveals superconvergence properties on the optimal grid. Another very important characteristic of the method is that if the differential operator and the metric coefficients are evaluated identically by some hybrid approximation the single optimal grid generator can be employed in the entire computational domain independently of points where the hybrid discretization switches from one approximation to another. Generalization of the present method to multiple dimensions is presented. Numerical calculations of several one-dimensional and one two-dimensional test examples demonstrate the performance of the method and corroborate the theoretical results.

Key words. truncation error, grid adaptation criterion, finite difference approximation, error equidistribution

Subject classification. Applied and Numerical Mathematics

1. Introduction. Grid adaptation has now become widespread for solving multi-dimensional partial differential equations in arbitrary-shaped domains. One of the most important problems associated with the adaptive grid generation is an essential effect of the grid point distribution on error in the numerical solution. Until the present time little attention has been paid to the fact that the concentration of grid points in regions which most influence the accuracy of the numerical solution may at the same time introduce additional error due to the grid non-uniformity [1]–[3].

There are two basic strategies of the grid adaptation, namely, grid refinement and grid redistribution techniques. In the first approach grid nodes are added to locally enrich the grid to achieve higher accuracy. In the second approach the number of grid nodes is fixed and the idea is to adjust the position of grid points to improve the numerical solution accuracy. In spite of significant distinctions, for both methods reliable and efficient grid adaptation criteria are needed.

A number of grid adaptation criteria based on the equidistribution principle have been developed. As has been shown in [4], the grid point distribution is asymptotically optimal if some error measure is equally distributed over the field. One of the widely-used approaches is to redistribute grid points in accordance with the arc length and the local curvature of the solution curve [5], [6]. This kind of clustering is intended to reduce the error in the vicinity of strong gradients and local extrema of the numerical solution, but it does not necessarily guarantee improvement in the accuracy where the solution is smooth.

Another class of methods is based on equidistribution or minimization of the local truncation error or its estimate [7]–[10]. In [7] the error estimate obtained by using a finite difference approximation of the

*Computational Modeling and Simulation Branch, Mail Stop 128, NASA Langley Research Center, Hampton, Virginia 23681-2199 (email: nail@tabdemo.larc.nasa.gov). This research was supported by the National Aeronautics and Space Administration under NASA Contract No. NAS1-97046 while the author was in residence at the Institute for Computer Applications in Science and Engineering (ICASE), NASA Langley Research Center, Hampton, Virginia 23681-2199

leading truncation error term is equidistributed by the grid point redistribution. Klopfer and McRae [8] solve a one-dimensional shock-tube problem using the explicit predictor-corrector scheme of MacCormack on a grid dynamically adapted to the solution. The error estimate is the leading truncation error term of the differential equations transformed to the computational coordinates. The metric coefficient is taken as a linear function of the smoothed error measure. For solving a second-order two-point boundary value problem with a centered second-order finite difference scheme Denny and Landis [9] suggest to determine the optimal coordinate mapping so that the entire truncation error vanishes at all grid points. However, this grid generator concentrates grid nodes where the solution is smooth rather than near steep gradients. Thus, the error reduction occurs in regions which do not practically affect the numerical solution accuracy. An alternative technique is employed in [10] where the optimal coordinate transformation is constructed as the solution of a constrained parameter optimization problem minimizing a measure of the truncation error. The error measure used is a finite difference evaluation of the third derivative of the numerical solution calculated in the computational space. The main drawback of all the methods mentioned above is the fact that the error estimates do not properly take into account that part of the truncation error which is caused by the nonuniform grid spacing. Furthermore, it is not clear how to extend these methods to more general equations and discretizations as well as to multiple dimensions.

A grid adaptation procedure equidistributing an error estimate of the numerical solution has successfully been used in [11] to reduce simulation error in such integral quantities as the lift or drag. This error estimate is directly related to the local residual errors of the primal and adjoint solutions of the Euler equations. As it follows from the numerical results presented in [11], the order of accuracy of the integral outputs increases by one if the proposed adaptation strategy is employed. Although, this approach provides significant improvement in the accuracy of the functional, the error estimation procedure is quite expensive in terms of computational time since except for the solution of the primal problem it is needed to solve the adjoint Euler equations that doubles the computational efforts.

The formulation of an adaptive mesh redistribution algorithm for boundary value problems in one dimension has been presented in [12]. The analysis uses the error minimization to produce an optimal piecewise-polynomial interpolant in a given norm that leads to the development of a family of grid adaptation criteria. Despite the fact that the present approach works well in one dimension this error equidistribution analysis can not be directly extended to multiple dimensions [13].

In [14] and [15] the finite element residual is applied to provide a criterion for determining where a finite element mesh requires refinement. As has been noted in [16] for hyperbolic problems with non-smooth solutions the finite element residual may be an ineffective error estimator since for such problems the residual measured in the L_2 norm diverges whereas the numerical solution converges in this norm. The problem might be overcome if the divergence of the residual is localized to the area of non-smoothness and the residual would then be used as a local error indicator. However, the localization of discontinuities becomes a very complicated problem in multiple dimensions.

It can be shown that the truncation error of any differential operator obtained on a nonuniform grid consists of two different parts. The first one, which always exists on a uniform mesh, is due to the approximation of the differential operator itself. The second one is caused by the contribution to the error from the nonuniform grid spacing. As the grid is locally refined or redistributed the first part of the error decreases while the second part may considerably increase because of the grid non-uniformity. All of the equidistribution methods mentioned above redistribute grid points in accordance with one or another error estimate obtained on a non-adapted grid, but in doing so the grid adaptation itself introduces additional

error which changes the error distribution. Therefore, to account for this change in the error distribution the grid adaptation procedure based on the error equidistribution strategy should be repeated iteratively until the error estimate norm is equally distributed over the field. Note that for moving meshes dynamically adapted to the solution the iterative procedure should be done at each time step to get the optimal mesh characterized by having the error equidistributed throughout the domain.

The main objective of this paper is to construct an optimal coordinate transformation so that the leading truncation error term of an arbitrary p th-order finite difference approximation is minimized that provides superconvergent results on the optimal grid. In contrast to the error equidistribution principle, for the present technique *a posteriori* error estimate is not explicitly required. Furthermore, the new grid adaptation criterion allows one to minimize the error due to the differential operator itself and the error owing to the evaluation of the metric coefficients simultaneously. Another very attractive feature of the present approach is its applicability to hybrid approximations which depend on some basic properties of the solution such as a flow direction, sonic line and others. If the metric coefficients are evaluated by the same hybrid discretization used for the differential operator, the new grid adaptation criterion remains valid in the whole computational domain regardless to points where the hybrid scheme switches from one approximation to another. Extension of the new adaptation criterion to multiple dimensions is presented. Numerical examples considered illustrate the ability of the method and corroborate the theoretical analysis.

2. Grid Adaptation in One Dimension. We consider the truncation error of the first derivative approximated on a 1D nonuniform grid. Let x and ξ denote the physical and computational coordinates, respectively. Without loss of generality it is assumed that $a \leq x \leq b$ and $0 \leq \xi \leq 1$. A one to one coordinate transformation between the physical and the computational domains is given by

$$(2.1) \quad x = x(\xi),$$

where

$$(2.2) \quad \begin{aligned} x(0) &= a \\ x(1) &= b. \end{aligned}$$

It is assumed that the above mapping is not singular so that the Jacobian of the transformation is a strictly positive function, i.e.

$$(2.3) \quad x_\xi > 0, \quad \forall \xi \in [0, 1].$$

The nonuniform grid in the physical space is obtained as images of nodes of a uniform mesh in the computational domain

$$(2.4) \quad x_i = x(\xi_i), \quad \xi_i = \frac{i}{I}, \quad i = 0, 1, \dots, I.$$

Taking into account the coordinate transformation Eq.(2.1) the first derivative of a function $f(x)$ with respect to x can be written as follows

$$(2.5) \quad f_x = \frac{f_\xi}{x_\xi}.$$

To construct a p th-order approximation of f_x in the physical domain we approximate f_ξ and x_ξ by some p th-order finite difference expressions in the computational domain

$$(2.6) \quad L_h(f_x) = \frac{\sum_{l=i-l_1}^{i+l_2} \alpha_l f_l}{\sum_{m=i-m_1}^{i+m_2} \beta_m x_m},$$

where $x_m = x(\xi_m)$, $f_l = f(\xi_l)$; L_h is a finite difference operator; the indexes l_1, l_2 and m_1, m_2 as well as the coefficients α_l and β_m depend on particular approximations used for evaluating f_ξ and x_ξ , respectively. Henceforth, we shall assume that the functions $f(\xi)$ and $x(\xi)$ are smooth enough so that all derivatives needed for the derivation are continuous functions on $\xi \in [0, 1]$. Expanding the nominator and denominator of Eq.(2.6) in a Taylor series with respect to ξ_i and omitting the index i on the right hand side yield

$$(2.7) \quad \begin{aligned} \sum_{l=i-l_1}^{i+l_2} \alpha_l f_l &= f_\xi + C_p^f f_\xi^{(p+1)} \Delta \xi^p + O(\Delta \xi^{p+1}) \\ \sum_{m=i-m_1}^{i+m_2} \beta_m x_m &= x_\xi + C_p^x x_\xi^{(p+1)} \Delta \xi^p + O(\Delta \xi^{p+1}), \end{aligned}$$

where

$$x_\xi^{(p+1)} = \frac{\partial^{p+1} x}{\partial \xi^{p+1}}, \quad f_\xi^{(p+1)} = \frac{\partial^{p+1} f}{\partial \xi^{p+1}}, \quad \Delta \xi = \frac{1}{I},$$

C_p^f and C_p^x are constants dependent on α_l and β_m , respectively. Substituting Eq.(2.7) into Eq.(2.6) and taking into account that $x_\xi > 0$, $\forall \xi \in [0, 1]$ one can write

$$(2.8) \quad L_h(f_x) = \frac{f_\xi + C_p^f \Delta \xi^p f_\xi^{(p+1)}}{x_\xi \left(1 + C_p^x \frac{\Delta \xi^p}{x_\xi} x_\xi^{(p+1)}\right)} + O(\Delta \xi^{p+1}).$$

Assuming that $\Delta \xi$ is chosen to be sufficiently small so that $\Delta \xi^p |x_\xi^{(p+1)}| / x_\xi \ll 1$, Eq.(2.7) can be linearized as follows

$$(2.9) \quad L_h(f_x) = \frac{1}{x_\xi} \left(f_\xi + C_p^f \Delta \xi^p f_\xi^{(p+1)} \right) \left(1 - C_p^x \frac{\Delta \xi^p}{x_\xi} x_\xi^{(p+1)} \right) + O(\Delta \xi^{p+1}).$$

Note that the error introduced by the linearization is of the order of $O(\Delta \xi^{2p+2})$. Neglecting higher order terms in Eq.(2.9) we have

$$(2.10) \quad T_p(x) = L_h(f_x) - f_x = C_p^f \Delta \xi^p \frac{f_\xi^{(p+1)}}{x_\xi} - C_p^x \Delta \xi^p \frac{x_\xi^{(p+1)}}{x_\xi^2} f_\xi.$$

The right hand side of Eq.(2.10) is the leading truncation error term. Thus, if the metric coefficient x_ξ is evaluated numerically as in Eq.(2.6) the asymptotic truncation error of any p th-order finite difference approximation consists of two different parts, one of which is due to the evaluation of f_ξ and the second one is caused by the discretization of the metric coefficient x_ξ . It should be emphasized that any grid adaptation based on minimization or equidistribution of the first part of the truncation error alone is not sufficient since the second part of the truncation error may drastically increase in regions where $x(\xi)$ rapidly changes. In other words, any inconsistent grid adaptation transfers the error from the first term of the truncation error to the second one and vice versa. To minimize both parts of the truncation error simultaneously we impose the following restriction on the coordinate mapping $x(\xi)$, $\forall \xi \in [0, 1]$

$$(2.11) \quad \left| C_p^f f_\xi^{(p+1)} x_\xi - C_p^x x_\xi^{(p+1)} f_\xi \right| \leq O(\Delta \xi) x_\xi^2.$$

If Eq.(2.11) holds the asymptotic order of approximation of Eq.(2.6)–(2.7) on the optimal grid generated by the mapping $x(\xi)$ is $p+1$ in the entire computational domain. Replacing the inequality sign by the equality one in Eq.(2.11) the grid adaptation criterion can be expressed as

$$(2.12) \quad C_p^f f_\xi^{(p+1)} x_\xi - C_p^x x_\xi^{(p+1)} f_\xi = O(\Delta \xi) x_\xi^2.$$

Recall that the coefficients C_p^f and C_p^x depend on the particular approximations used and do not depend on $f(\xi)$ and $x(\xi)$. One of the most important classes of approximation is a consistent approximation when the same difference operator is employed to evaluate the derivatives f_ξ and x_ξ . In this case the coefficients C_p^f and C_p^x are identical and Eq.(2.12) is simplified to

$$(2.13) \quad f_\xi^{(p+1)} - f_x x_\xi^{(p+1)} = O(\Delta\xi)x_\xi$$

or setting the right hand side equal to zero yields

$$(2.14) \quad f_\xi^{(p+1)}x_\xi - f_x x_\xi^{(p+1)} = 0.$$

There are several advantages of such a simplification. First of all, the use of the same difference approximation for both f_ξ and x_ξ eliminates the f_x term from the truncation error which is the most troublesome part of the error being dependent on the first derivative which is evaluated. Actually, let us represent f_ξ and $f_\xi^{(p+1)}$ in terms of the x derivatives

$$(2.15) \quad \begin{aligned} f_\xi &= x_\xi f_x \\ f_\xi^{(p+1)} &= \left(\frac{\partial}{\partial \xi} + x_\xi \frac{\partial}{\partial x} \right)^{p+1} f = x_\xi^{(p+1)} f_x + (p+1)x_\xi^{(p)} x_\xi f_{xx} + \dots + x_\xi^{p+1} f_x^{(p+1)} \end{aligned}$$

Note that the binomial theorem can not be used to expand the power of the derivative operator in the above formula since $\partial/\partial\xi$ and $x_\xi\partial/\partial x$ do not commute. Substituting the above expressions into Eq.(2.10) the leading term of the truncation error $T_p(x)$ can be written as follows

$$(2.16) \quad T_p(x) = (C_p^f - C_p^x)\Delta\xi^p \frac{x_\xi^{(p+1)}}{x_\xi} f_x + C_p^f \left[(p+1)x_\xi^{(p)} f_{xx} + \dots + x_\xi^p f_x^{(p+1)} \right]$$

From Eq.(2.16) it is clear that if $C_p^f \neq C_p^x$ then the truncation error depends on the first derivative f_x being approximated. That is why it is very important to evaluate the metric coefficient by the same difference approximation used for f_ξ . It should be noted, that if x_ξ is approximated by the exact analytical expression or any finite difference formula different from that which is employed to calculate f_ξ it gives rise to the f_x term in the truncation error.

Another advantage of the consistent approximation of f_ξ and x_ξ is that the single optimal grid in the sense of Eq.(2.14) can be generated for hybrid discretization, when the coefficient C_p^f may implicitly depend on the function $f(\xi)$. The identical numerical approximation of x_ξ and f_ξ removes the dependence of the optimal mapping on points in the physical domain where the hybrid scheme switches from one approximation to another. If this is the case the optimal grid point distribution depends only on the order of approximation and is completely independent of the particular finite difference formula used.

As has already been mentioned, Eq.(2.14) is a grid adaptation criterion, but at the same time this equation can be treated as a grid generation equation. To provide the existence of the solution of Eq.(2.14) it is assumed that $f_\xi > \epsilon > 0$, $\forall \xi \in [0, 1]$, and $f(\xi) \in C^{p+1}[0, 1]$. It can easily be seen that $x(\xi) = c_1 f(\xi) + c_2$ is the solution of Eq.(2.14), but this trivial solution is not appropriate since it means that $f(x)$ is a linear function of x in the physical space. Another problem associated with the solution of Eq.(2.14) is boundary conditions. Theoretically, to find the unique solution of Eq.(2.14) $p+1$ boundary conditions should be imposed while only two boundary conditions Eq.(2.2) are available. In spite on the abovementioned difficulties the optimal grid generation problem Eqs.(2.14),(2.2) can be solved analytically for very important cases $p = 1, 2$ and the approximate analytical solutions can be obtained for higher order discretizations $p \geq 3$.

2.1. First-Order Approximation, $p = 1$. For a first-order accurate approximation p is equal to one in Eq.(2.13) which takes the form

$$(2.17) \quad f_{\xi\xi}x_\xi - f_\xi x_{\xi\xi} = O(\Delta\xi)x_\xi^2.$$

Using the following expression for the second derivative

$$f_{xx} = \frac{f_{\xi\xi}x_\xi - f_\xi x_{\xi\xi}}{x_\xi^3}$$

Eq.(2.17) written in the physical space is reduced to

$$(2.18) \quad \xi_x = \frac{f_{xx}}{O(\Delta\xi)}.$$

Integrating Eq.(2.18) and taking into account the boundary conditions $\xi(a) = 0$, $\xi(b) = 1$ yield

$$(2.19) \quad \xi(x) = \frac{\int_a^x f_{xx} dx}{\int_a^b f_{xx} dx}.$$

However, to satisfy Eq.(2.18) the following restriction should be imposed on f_{xx}

$$(2.20) \quad \int_a^b f_{xx} dx = O(\Delta\xi).$$

Since $\xi_x > 0$ from Eq.(2.18) it follows that $f_{xx} > 0$. Consequently, Eq.(2.20) means that the second derivative f_{xx} has to be of the order of $O(\Delta\xi)$ for all $x \in [a, b]$. In other words, if $f(x)$ is an essentially nonlinear function, so that Eq.(2.20) is not satisfied, it is impossible to increase the global order of accuracy of f_x by the grid point redistribution.

2.2. Second-Order Approximation, $p = 2$. If both f_ξ and x_ξ are evaluated identically by a second-order accurate formula the grid adaptation equation Eq.(2.13) written for $p = 2$ becomes

$$(2.21) \quad f_{\xi\xi\xi}x_\xi - f_\xi x_{\xi\xi\xi} = O(\Delta\xi)x_\xi^2$$

Let us transform the derivatives in Eq.(2.21) from the computational space to the physical space

$$(2.22) \quad \begin{aligned} f_\xi &= f_x x_\xi \\ f_{\xi\xi\xi} &= f_{xxx}x_\xi^3 + 3f_{xx}x_\xi x_{\xi\xi} + f_x x_{\xi\xi\xi}. \end{aligned}$$

Substituting Eq.(2.22) into Eq.(2.21) we have

$$(2.23) \quad f_{xxx}x_\xi^2 + 3f_{xx}x_{\xi\xi} = O(\Delta\xi)x_\xi^2$$

Using the following expressions for the metric coefficient and its derivative

$$\begin{aligned} x_\xi &= \frac{1}{\xi_x} \\ x_{\xi\xi} &= -\frac{\xi_{xx}}{\xi_x^3} \end{aligned}$$

and assuming that $f_{xx} \neq 0, \forall x \in [a, b]$ Eq.(2.23) can be rewritten as

$$(2.24) \quad \frac{f_{xxx}}{f_{xx}} = 3\frac{\xi_{xx}}{\xi_x} + O(\Delta\xi)\frac{\xi_x^2}{f_{xx}}$$

Since a decrease in the last term in the above equation increases the approximation accuracy we neglect the $O(\Delta\xi)$ term and integrate the left and right hand sides of Eq.(2.24) with respect to x to give

$$(2.25) \quad \xi_x^3 = C f_{xx},$$

where C is a constant of the integration. Equation (2.25) has one real and two complex roots. Since we seek only real roots the complex roots are not considered. Taking into account the boundary conditions Eq.(2.2) the above equation can readily be integrated, that gives

$$(2.26) \quad \xi(x) = \frac{\int_a^x (f_{xx})^{1/3} dx}{\int_a^b (f_{xx})^{1/3} dx}.$$

If a grid is generated in accordance with the optimal mapping Eq.(2.26) the leading term of the truncation error is zero for all points in $[a, b]$ and the global order of accuracy is increased from 2 to 3.

The optimal grid point distribution defined by Eq.(2.26) can be applied if f_{xx} is a positive function otherwise the mapping becomes singular that leads to the grid degeneration. However, this problem can be overcome. For that purpose we divide the interval $[a, b]$ on subintervals where f_{xx} is of constant signs. Let $x_1^- < x < x_2^-$ be an interval where the second derivative is negative, i.e. $f_{xx} = -|f_{xx}| < 0$. Then, Eq.(2.26) becomes

$$(2.27) \quad \xi(x) = \frac{\int_{x_1^-}^x (f_{xx})^{1/3} dx}{\int_{x_1^-}^{x_2^-} (f_{xx})^{1/3} dx} = \frac{-\int_{x_1^-}^x |f_{xx}|^{1/3} dx}{-\int_{x_1^-}^{x_2^-} |f_{xx}|^{1/3} dx} = \frac{\int_{x_1^-}^x |f_{xx}|^{1/3} dx}{\int_{x_1^-}^{x_2^-} |f_{xx}|^{1/3} dx}$$

From Eq.(2.27) it follows that the metric coefficient ξ_x given by Eq.(2.26) is strictly positive in the interval where f_{xx} is negative. Taking into account the fact that the same formula Eq.(2.27) remains valid for positive f_{xx} the intervals of positive and negative signs except for the inflection points of the function $f(x)$ can be joined so that

$$(2.28) \quad \xi(x) = \frac{\sum_j \int_{x_{j+0}}^x |f_{xx}|^{1/3} dx}{\sum_j \int_{x_{j+0}}^{x_{j+1-0}} |f_{xx}|^{1/3} dx}, \quad \forall x : x \neq x_j,$$

where x_j are the inflection points of $f(x)$. To add the inflection points $f_{xx}(x_j) = 0$ to the above integrals special consideration is required.

Let x_0 be a point of inflection of the function $f(x)$, i.e. $f_{xx}(x_0) = 0$. Note in passing that if we modify the function $f(x)$ by adding an arbitrary linear function the optimal grid Eq.(2.26) remains unchanged. Furthermore, if the function $f(x)$ is linear in the whole interval $[a, b]$ then from Eq.(2.25) it follows that $\xi_x = 0$, $\forall x \in [a, b]$. It results in that the grid step size in the physical domain $\Delta x = \Delta\xi/\xi_x$ tends to infinity. It can be interpreted as to approximate the first derivative of the linear function exactly an arbitrary large grid spacing can be used. Expanding f_{xx} in a Taylor series about $x = x_0$ in Eq.(2.26) and assuming that $f_{xxx}(x_0) \neq 0$ yield

$$f_{xx}(x) = f_{xxx}(x_0)(x - x_0) + O((x - x_0)^2)$$

Substituting the above expression in Eq.(2.26) and neglecting both $O((x-x_0)^2)$ and higher order terms give

$$(2.29) \quad \xi_x^3 = C f_{xxx}(x_0)(x-x_0)$$

Letting $x \rightarrow x_0$ we have

$$\xi_x(x_0) = \lim_{x \rightarrow x_0} (C f_{xxx}(x_0)(x-x_0))^{1/3} = 0$$

As noted above, this kind of grid degeneration when the metric coefficient ξ_x vanishes does not impose any restriction on the grid step size at the inflection point. Therefore, in the vicinity of the inflection point the original second derivative f_{xx} can be modified as

$$(2.30) \quad \tilde{f}_{xx}(x) = \begin{cases} |f_{xx}|, & |f_{xx}| \geq \epsilon \\ \frac{(f_{xx})^2 + \epsilon^2}{2\epsilon}, & |f_{xx}| < \epsilon \end{cases}$$

where ϵ is a small positive parameter. From the above consideration it follows that for an arbitrary $f \in C^2[a, b]$ the optimal mapping minimizing the leading truncation error term globally is

$$(2.31) \quad \tilde{\xi}(x) = \frac{\int_a^x (\tilde{f}_{xx})^{1/3} dx}{\int_a^b (\tilde{f}_{xx})^{1/3} dx}.$$

To estimate the asymptotic truncation error of the second-order difference expression for f_x on the optimal grid Eq.(2.26) we rewrite Eq.(2.8) including the third-order terms

$$(2.32) \quad L_h(f_x) = \frac{f_\xi + C_2 \Delta \xi^2 f_{\xi\xi\xi} + C_3 \Delta \xi^3 f_\xi^{(4)}}{x_\xi + C_2 \Delta \xi^2 x_{\xi\xi\xi} + C_3 \Delta \xi^3 x_\xi^{(4)}} + O(\Delta \xi^4).$$

Linearizing Eq.(2.32) and collecting the terms of $O(\Delta \xi^2)$ and $O(\Delta \xi^3)$ the first two leading terms in the truncation error are

$$(2.33) \quad T_2(x) = C_2 \frac{\Delta \xi^2}{x_\xi^2} [f_{\xi\xi\xi} x_\xi - x_{\xi\xi\xi} f_\xi] + C_3 \frac{\Delta \xi^3}{x_\xi^2} [f_\xi^{(4)} x_\xi - x_\xi^{(4)} f_\xi].$$

Since the first term on the right hand side of Eq.(2.33) is vanished on the optimal grid defined by Eq.(2.26) the asymptotic truncation error becomes

$$(2.34) \quad T_2(x) = C_3 \frac{\Delta \xi^3}{x_\xi^2} [f_\xi^{(4)} x_\xi - x_\xi^{(4)} f_\xi].$$

To determine the expression in the square brackets we differentiate Eq.(2.14) written for $p = 2$ with respect to ξ . Thus,

$$(2.35) \quad f_\xi^{(4)} x_\xi + f_{\xi\xi\xi} x_{\xi\xi\xi} - f_{\xi\xi} x_{\xi\xi\xi\xi} - x_\xi^{(4)} f_\xi = 0.$$

Resolving Eq.(2.14) with respect to $f_{\xi\xi\xi}$ and substituting it in Eq.(2.35) give

$$(2.36) \quad f_\xi^{(4)} x_\xi - x_\xi^{(4)} f_\xi = x_{\xi\xi\xi} x_\xi^2 f_{xx}.$$

Using Eq.(2.36) the leading truncation error term on the optimal grid Eq.(2.26) can be recast as

$$(2.37) \quad T_2(x) = C_3 \Delta \xi^3 x_{\xi\xi\xi} f_{xx}.$$

Taking into account the fact that for the optimal grid Eq.(2.26) holds, $x_{\xi\xi\xi}$ can be represented in terms of the function $f(x)$ and its derivatives as follows

$$(2.38) \quad x_{\xi\xi\xi} = \frac{3\xi_{xx}^2 - \xi_{xxx}\xi_x}{\xi_x^5} = \frac{5f_{xxx}^2 - 3f_x^{(4)}f_{xx}}{9C^3f_{xx}^3},$$

where C is the integration constant in Eq.(2.25). Substituting Eq.(2.38) into Eq.(2.37) the leading truncation error term is given by

$$(2.39) \quad T_2(x) = C_3\Delta\xi^3 \frac{5f_{xxx}^2 - 3f_x^{(4)}f_{xx}}{9C^3f_{xx}^2}.$$

This formula is valid for all points from the interval $[a, b]$ except for the inflection points of the function $f(x)$.

Let us estimate the leading term of the truncation error at a point of inflection $x_0 : f_{xx}(x_0) = 0$. Since we have modified the second derivative f_{xx} in the neighborhood of the inflection point Eq.(2.30) the second-order term in the truncation error does not vanish. Substituting Eq.(2.30) into Eq.(2.33) and neglecting higher order terms we have

$$T_2(x_0) = C_2\Delta\xi^2 \frac{-f_{xx}\tilde{f}_{xxx}(\tilde{f}_{xx})^{-2/3} + (\tilde{f}_{xx})^{1/3}f_{xxx}}{\tilde{f}_{xx}}.$$

Letting $x \rightarrow x_0$ yields

$$(2.40) \quad T_2(x_0) = C_2\Delta\xi^2 \frac{f_{xxx}(x_0)}{(\epsilon/2)^{2/3}}.$$

Equation (2.40) shows that, locally, near the inflection point only the second order of approximation can be obtained on the optimal grid. Note that it is not the case if the function $f(x)$ is linear because then, any second-order accurate approximation of f_ξ and x_ξ in Eq.(2.5) on an arbitrary nonuniform mesh gives us the exact value of f_x . By virtue of the fact that the number of the inflection points is finite the L_2 norm of the second-order accurate approximation of f_x on the optimal grid should provide superconvergent results.

In regions where the function $f(x)$ is discontinuous the above reasoning is not valid since the first and higher derivatives do not exist there. In contrast to the inflection point in the vicinity of local extrema of $f(x)$, where \tilde{f}_{xx} achieves its maximum value, the fraction in Eq.(2.39) becomes very small so that locally, even a higher order of accuracy may be obtained.

Remark 2.1 It can readily be checked that standard grid adaptation criteria such as the arc length of the function $f(x)$ and the second derivative f_{xx} do not globally minimize the leading term of the truncation error. Actually, using the arc length grid adaptation criterion the following grid point distribution is obtained

$$(2.41) \quad \xi(x) = \frac{\int_a^x \sqrt{1+f_x^2} dx}{\int_a^b \sqrt{1+f_x^2} dx}$$

Substituting Eq.(2.41) into Eq.(2.33) yields

$$(2.42) \quad T_2(x) = C_2\Delta\xi^2 \frac{-3f_x f_{xx}^2 + (1+f_x^2)f_{xxx}}{(1+f_x^2)^2}.$$

The comparison of Eq.(2.42) with the leading term of the truncation error obtained on a uniform grid, which is

$$T_2^{un}(x) = C_2\Delta\xi^2 f_{xxx},$$

shows that this grid point distribution may improve the accuracy locally near steep gradients of the function $f(x)$. At the same time, in regions where f_{xx} is much greater than f_x , e.g. near local extrema of $f(x)$, the actual order of approximation may deteriorate to one or even be worse.

If instead of the arc length adaptation criterion one redistributes grid points in accordance with the second derivative f_{xx} the leading term of the truncation error is

$$(2.43) \quad T_2(x) = -C_2 \Delta \xi^2 \frac{2f_{xxx}}{f_{xx}^2}.$$

As it follows from the above formula in regions where $|f_{xx}| < \sqrt{2}$ the local truncation error Eq.(2.43) is always greater than the asymptotic truncation error on a uniform grid.

Summarizing what has been said above the following conclusions can be drawn. On the one hand, the standard grid adaptation criteria do not provide the superconvergence. On the other hand, although, the standard grid adaptation techniques may locally improve the accuracy of calculation the global truncation error may become even larger than that obtained on the corresponding uniform mesh. Despite the fact that the above consideration has been performed for the second-order discretization the same conclusion can be done for higher order schemes.

Remark 2.2 We shall now briefly describe an alternative way of the solution of Eq.(2.21). Integrating Eq.(2.21) by parts and neglecting the $O(\Delta \xi)$ term on the right hand side yield

$$(2.44) \quad f_{\xi\xi} x_\xi - f_\xi x_{\xi\xi} = C,$$

where C is a constant of the integration. The above equation is closed by using the boundary conditions Eq.(2.2).

In order to find the unknown constant C we rewrite Eq.(2.44) in the following form

$$(2.45) \quad x_\xi^2 \frac{\partial}{\partial \xi} \left(\frac{f_\xi}{x_\xi} \right) = C,$$

Taking into account the fact that

$$f_{xx} = \frac{1}{x_\xi} \frac{\partial}{\partial \xi} \left(\frac{f_\xi}{x_\xi} \right)$$

Eq.(2.45) is reduced to Eq.(2.25) and the constant C can easily be determined, that gives

$$(2.46) \quad C = \left(\int_a^b (f_{xx})^{1/3} dx \right)^3.$$

The boundary value problem Eq.(2.44),(2.46),(2.2) should be solved numerically. If at some point f_ξ and $f_{\xi\xi}$ are equal to zero simultaneously Eq.(2.44),(2.46) is degenerated. The problem can be overcome by modifying the derivatives f_ξ , $f_{\xi\xi}$ and the constant C as follows

$$\tilde{f}_\xi = \frac{\tilde{f}_x}{\tilde{\xi}_x} = \frac{\tilde{f}_x}{(\tilde{C} \tilde{f}_{xx})^{1/3}}$$

$$\tilde{f}_{\xi\xi} = \frac{\tilde{f}_{xx} \tilde{\xi}_x - \tilde{\xi}_{xx} \tilde{f}_x}{\tilde{\xi}_x^3} = \frac{3(\tilde{f}_{xx})^2 - \tilde{f}_{xxx} \tilde{f}_x}{\tilde{C}^{2/3} (\tilde{f}_{xx})^{5/3}}$$

$$\tilde{C} = \left(\int_a^b (\tilde{f}_{xx})^{1/3} dx \right)^3,$$

where \tilde{f}_{xx} is given by Eq.(2.30), \tilde{f}_x and \tilde{f}_{xxx} are calculated by differentiating and integrating \tilde{f}_{xx} with respect to x , accordingly. Since the function \tilde{f}_{xx} is strictly positive in the entire computational domain the first derivative \tilde{f}_x is a positive function as well. It makes the modified equation fully consistent with Eq.(2.31).

It should be stressed that there are several differential forms of the optimal grid generation equation. For example, instead of integration of Eq.(2.21) by parts we may consider Eq.(2.23) as a differential equation for the optimal grid point distribution. Since each of the differential equations has its advantages and disadvantages at the present time, it is difficult to say which one of them is better.

2.3. High-Order Approximations, $p \geq 3$. If f_ξ and x_ξ are approximated identically by a third-order accurate formula the optimal grid generation equation written in operator form in the physical space is

$$(2.47) \quad \left[\frac{1}{\xi_x} \frac{\partial}{\partial x} \right]^4 f - f_x \left[\frac{1}{\xi_x} \frac{\partial}{\partial x} \right]^4 x = 0.$$

Performing the indicated differentiation we have

$$(2.48) \quad f_{xx} (15\xi_{xx}^2 - 4\xi_x \xi_{xxx}) + \xi_x \left(-6\xi_{xx} f_{xxx} + \xi_x f_x^{(4)} \right) = 0$$

Although, the above equation is much more complicated than the analogous one derived for the second-order discretizations Eq.(2.24) we shall construct the solution of Eq.(2.48) in a similar form. On the one hand, a solution in the form of $\xi = g(f_x)$, where g is an arbitrary function of f_x , is not appropriate since in this case the $f_x^{(4)}$ term in Eq.(2.48) can not be canceled. On the other hand, if a solution depends on f_{xxx} or higher derivatives of $f(x)$ it gives rise to the $f_x^{(5)}$ term in the truncation error which is not canceled as well. Therefore, we shall seek the solution of Eq.(2.48) in a form similar to Eq.(2.25)

$$(2.49) \quad \xi_x = C(f_{xx})^\alpha.$$

Substituting Eq.(2.49) into Eq.(2.48) the leading truncation error term can be written as

$$(2.50) \quad T_3(x) = \frac{C_3 \Delta \xi^3}{(f_{xx})^{1+2\alpha}} \left[\alpha(2 - 11\alpha)(f_{xxx})^2 + (4\alpha - 1)f_{xx} f_x^{(4)} \right]$$

In contrast to the second-order discretization, for the third-order approximation the leading term of the truncation error does not vanish at any $\alpha = const$. Assuming that the parameter $\alpha(x)$ is a function which weakly depends on x and setting the leading truncation error term equal to zero the following quadratic equation for $\alpha(x)$ is obtained

$$(2.51) \quad \alpha(x)(2 - 11\alpha(x))(f_{xxx})^2 + (4\alpha(x) - 1)f_{xx} f_x^{(4)} = 0$$

The solution of Eq.(2.51) is

$$(2.52) \quad \alpha_{1,2} = \frac{1}{11} \left(1 + 2r(x) \pm \sqrt{1 - 7r(x) + 4r(x)^2} \right),$$

with

$$r(x) = \frac{f_{xx} f_x^{(4)}}{(f_{xxx})^2}.$$

Without loss of generality it is assumed that $f_{xxx} \neq 0$. If $f_{xxx} = 0$ then the solution of Eq.(2.51) is $\alpha = 1/4$. Note that the function $\alpha(x)$ should be positive in the entire physical domain otherwise, the mapping Eq.(2.49) with $\alpha < 0$ concentrates grid points where $f(x)$ is linear and makes the grid very coarse where the second derivative f_{xx} is large. Since the above analysis is valid if the function $\alpha(x)$ slightly depends on x we construct α as follows

$$(2.53) \quad \alpha(r) = \begin{cases} \frac{1}{11} (1 + 2r + \sqrt{1 - 7r + 4r^2}), & r \leq 0 \\ -\frac{48}{343}r^3 + \frac{18}{49}r^2 - \frac{3}{22}r + \frac{2}{11}, & 0 < r < \frac{7}{4} \\ \frac{1}{11} (1 + 2r - \sqrt{1 - 7r + 4r^2}), & r \geq \frac{7}{4} \end{cases}$$

where the polynomial in Eq.(2.53) has been chosen so that $\alpha(r)$ is a continuously differentiable function of r . A plot of α versus r is shown in Fig.2.1. As can be seen in the figure, the function $\alpha(r)$ is practically equal to $1/4$ in the whole range of r except for an interval $-1 \leq r \leq 3$. Although, $\alpha(r)$ is quite smooth the function $\alpha(x)$ may be non-smooth because it depends on f_{xx} , f_{xxx} and $f_x^{(4)}$ which are calculated numerically and may therefore be very oscillatory. In numerical applications the function $\alpha(x)$ should be smoothed to meet the requirements used for the derivation of Eq.(2.50).

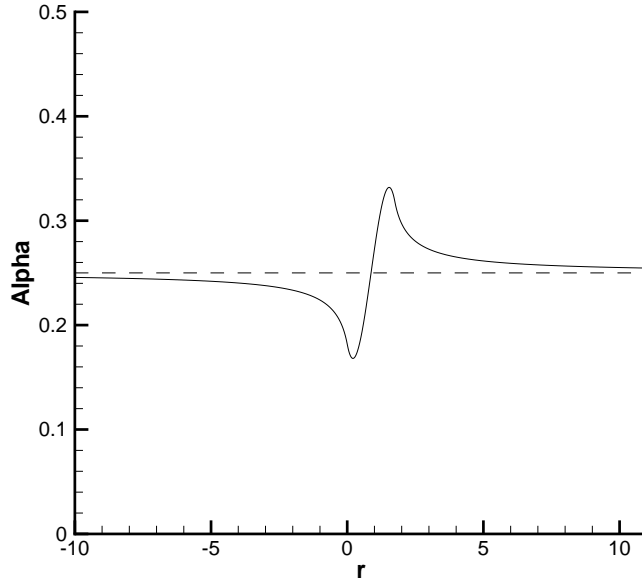


FIG. 2.1. Parameter α for a third-order accurate discretization.

Such a choice of $\alpha(x)$ provides that the leading truncation error term is approximately equal to zero in the entire physical domain. As it follows from Eq.(2.49), the second derivative f_{xx} must be a positive function on $[a, b]$. Note that a general property of both Eq.(2.47) and Eq.(2.14) is that if ξ_x is a solution of Eq.(2.47) then $-\xi_x$ is a solution of Eq.(2.47) as well. The same is true for the function $f(x)$ and its derivatives, i.e. if we substitute $\hat{f}_{xx} = -f_{xx}$ into Eq.(2.47) we get the same equation in terms of \hat{f}_{xx} . Hence, the second derivative f_{xx} in Eq.(2.49) can be replaced with Eq.(2.30). Thus, if f_ξ and x_ξ are evaluated by the same third-order accurate formula the optimal grid point distribution, which minimizes the leading term

of the truncation error in the entire computational domain, is

$$(2.54) \quad \xi(x) = \frac{\int_a^x (\tilde{f}_{xx})^{\alpha(x)} dx}{\int_a^b (\tilde{f}_{xx})^{\alpha(x)} dx},$$

where \tilde{f}_{xx} and $\alpha(x)$ are defined by Eq.(2.30) and Eq.(2.53), respectively.

From the above analysis one can see that the same strategy used for the third-order approximation can be applied to higher order discretizations. Actually, the leading term of the truncation error for an arbitrary p th-order approximation of f_x is

$$(2.55) \quad T_p(\xi) = \frac{C_p \Delta \xi^p}{x_\xi^2} \left(f_\xi^{(p+1)} x_\xi - f_\xi x_\xi^{(p+1)} \right)$$

Accounting for the following relations between the ξ - and x -derivatives written in operator form

$$\frac{\partial}{\partial \xi} = \frac{1}{\xi_x} \frac{\partial}{\partial x}$$

$$\frac{\partial^n}{\partial \xi^n} = \left[\frac{1}{\xi_x} \frac{\partial}{\partial x} \right]^n$$

the truncation error can be transformed into the physical space as follows

$$(2.56) \quad T_p(x) = C_p \Delta \xi^p \xi_x \left(\left[\frac{1}{\xi_x} \frac{\partial}{\partial x} \right]^{p+1} f - f_x \left[\frac{1}{\xi_x} \frac{\partial}{\partial x} \right]^{p+1} x \right).$$

Expanding the power of the derivative operator

$$(2.57) \quad \begin{aligned} \left[\frac{1}{\xi_x} \frac{\partial}{\partial x} \right]^{p+1} f &= \left[\left[\frac{1}{\xi_x} \frac{\partial}{\partial x} \right] x \frac{\partial}{\partial x} \right]^{p+1} = \\ &= \left[\frac{1}{\xi_x} \frac{\partial}{\partial x} \right]^{p+1} x \frac{\partial f}{\partial x} + (p+1) \left[\frac{1}{\xi_x} \frac{\partial}{\partial x} \right]^p x \left[\frac{1}{\xi_x} \frac{\partial}{\partial x} \right] \frac{\partial f}{\partial x} + \dots + \left[\frac{1}{\xi_x} \frac{\partial}{\partial x} \right] x \left[\frac{1}{\xi_x} \frac{\partial}{\partial x} \right]^p \frac{\partial f}{\partial x} \end{aligned}$$

it can be seen that the term with f_x in Eq.(2.56) is canceled and therefore the highest derivatives of $\xi(x)$ and $f(x)$ in the truncation error $T_p(x)$ are $\xi_x^{(p)}$ and $f_x^{(p+1)}$, respectively. Assuming that on the optimal grid the leading term of the truncation error is of the order of $O(\Delta \xi)$ we shall seek $\xi(x)$ as a function of $f(x)$ and its derivatives. Comparing the highest derivatives of ξ and f one can observe that if $\xi_x = g(f, f_x)$ then the term $f_x^{(p+1)}$ in Eq.(2.57) is never canceled while if ξ_x is a function of $f_x^{(n)}$, $n \geq 3$ it introduces the uncancellable $f_x^{(n+p-1)}$ term in the truncation error $T_p(x)$. In a similar manner to the first-, second-, and third-order approximations the optimal grid for the p th-order accurate discretization is sought in the form of Eq.(2.49). Substituting Eq.(2.49) into Eq.(2.57) the leading truncation error term becomes

$$(2.58) \quad T_p(x) = \frac{C_p \Delta \xi^p}{(f_{xx})^{p\alpha}} \left([1 - \alpha(p+1)] f_x^{(p+1)} + \alpha G(\alpha, f_{xx}, f_{xxx}, \dots, f_x^{(p)}) \right)$$

In the above formula it has already been taken into account that the second term on the right hand side is proportional to α . This is no surprise since for $\alpha = 0$, which corresponds to a uniform mesh, the asymptotic truncation error $T_p(x)$ is reduced to $C_p \Delta \xi^p f_x^{(p+1)}$ that is why all the terms in Eq.(2.58) except for $f_x^{(p+1)}$ have to be proportional to α . For example, for fourth- and fifth-order discretizations the leading truncation error terms obtained on the optimal grid Eq.(2.49) are

$$(2.59) \quad T_4(x) = \frac{C_4 \Delta \xi^4}{(f_{xx})^{4\alpha}} \left((1 - 5\alpha) f_x^{(5)} + \alpha \left\{ -10\alpha(1 + 5\alpha) \frac{(f_x^{(3)})^3}{(f_{xx})^2} + 5(9\alpha - 1) \frac{f_x^{(3)} f_x^{(4)}}{f_{xx}} \right\} \right)$$

and

$$(2.60) \quad T_5(x) = \frac{C_5 \Delta \xi^5}{(f_{xx})^5 \alpha} \left((1 - 6\alpha) f_x^{(6)} + \alpha \left\{ (6 + 49\alpha + 196\alpha^2 + 274\alpha^3) \frac{(f_x^{(3)})^4}{(f_{xx})^3} - \right. \right. \\ \left. \left. - (7 + 97\alpha + 421\alpha^2) \frac{(f_x^{(3)})^2 f_x^{(4)}}{(f_{xx})^2} + 3(27\alpha - 2) \frac{f_x^{(3)} f_x^{(5)}}{f_{xx}} + 2(26\alpha - 1) \frac{(f_x^{(4)})^2}{f_{xx}} \right\} \right),$$

respectively. As it follows from Eq.(2.58) at any $\alpha = \text{const}$ both terms on the right hand side do not vanish simultaneously. To minimize the leading term of the truncation error the following procedure is proposed. At each grid point the parameter α is found as the solution of the nonlinear equation $T(\alpha) = 0$, which is solved by the Newton's method. That choice of α provides that the leading truncation error term is vanished on the optimal grid. Since the above consideration is valid only if α slightly depends on x the function $\alpha(x)$ has to be smoothed in numerical applications.

Remark 2.3 If $p \rightarrow +\infty$, i.e. the order of approximation is infinitely large the leading term of the truncation error Eq.(2.58) is vanished for $\alpha \rightarrow 0$. In other words, the higher is the order of approximation used to evaluate f_ξ and x_ξ the more uniform is the grid which minimizes the leading truncation error term. In the limit of infinitely high-order approximations a uniform grid is optimal in the sense of minimization of the asymptotic truncation error.

3. Grid Adaptation in Multiple Dimensions. The two-dimensional transformation of the first derivative is given by

$$(3.1) \quad f_x = \frac{y_\eta f_\xi - y_\xi f_\eta}{J},$$

where the Jacobian of the transformation is

$$J = x_\xi y_\eta - x_\eta y_\xi.$$

Approximating the ξ and η derivatives in Eq.(3.1) by some p th- and q th-order finite difference formulas, respectively, we get

$$(3.2) \quad L_h(f_x) = \frac{(y_\eta + C_q \Delta \eta^q y_\eta^{(q+1)})(f_\xi + C_p \Delta \xi^p f_\xi^{(p+1)}) - (y_\xi + C_p \Delta \xi^p y_\xi^{(p+1)})(f_\eta + C_q \Delta \eta^q f_\eta^{(q+1)})}{(x_\xi + C_p \Delta \xi^p x_\xi^{(p+1)})(y_\eta + C_q \Delta \eta^q y_\eta^{(q+1)}) - (x_\eta + C_q \Delta \eta^q x_\eta^{(q+1)})(y_\xi + C_p \Delta \xi^p y_\xi^{(p+1)})} + O(\Delta \xi^{p+1}, \Delta \eta^{q+1})$$

In the above expression it has already been taken into account that the metric coefficients x_ξ, y_ξ and x_η, y_η are evaluated by the same finite difference operators which are used for calculating f_ξ and f_η , respectively.

In view of the fact that the mapping used is nonsingular $J > 0$, the denominator of Eq.(3.2) can be linearized that yields

$$(3.3) \quad L_h(f_x) = \frac{1}{J} \left[y_\eta f_\xi - y_\xi f_\eta + C_p \Delta \xi^p (y_\eta f_\xi^{(p+1)} - y_\xi^{(p+1)} f_\eta) + C_q \Delta \eta^q (f_\xi y_\eta^{(q+1)} - y_\xi f_\eta^{(q+1)}) \right] \times \\ \left[1 - \frac{C_p \Delta \xi^p}{J} (y_\eta x_\xi^{(p+1)} - y_\xi^{(p+1)} x_\eta) - \frac{C_q \Delta \eta^q}{J} (x_\xi y_\eta^{(q+1)} - y_\xi x_\eta^{(q+1)}) \right] + O(\Delta \xi^{p+1}, \Delta \eta^{q+1})$$

Multiplying out the terms in the square brackets and neglecting higher order terms the leading term of truncation error becomes

$$(3.4) \quad T_{p,q}(\xi, \eta) = \frac{1}{J} \left\{ C_p \Delta \xi^p \left[y_\eta f_\xi^{(p+1)} - y_\xi^{(p+1)} f_\eta - f_x (y_\eta x_\xi^{(p+1)} - x_\eta y_\xi^{(p+1)}) \right] + \right. \\ \left. + C_q \Delta \eta^q \left[f_\xi y_\eta^{(q+1)} - y_\xi f_\eta^{(q+1)} - f_x (x_\xi y_\eta^{(q+1)} - y_\xi x_\eta^{(q+1)}) \right] \right\}$$

As in the 1D case, the truncation error $T_{p,q}$ consists of two different parts, one of which arises from the evaluation of the metric coefficients $x_\xi, y_\xi, x_\eta, y_\eta$ and the second one occurs due to the approximation of f_ξ

and f_η . From Eq.(3.4) it follows that if the absolute value of the first expression in the square brackets is less than $O(\Delta\xi)$ and the absolute value of the second one is less than $O(\Delta\eta)$ then the global truncation error is $O(\Delta\xi^{p+1}, \Delta\eta^{q+1})$ rather than $O(\Delta\xi^p, \Delta\eta^q)$. Thus, to increase the order of the finite difference approximation Eq.(3.2) by one globally grid points should be redistributed so that the following equations hold

$$(3.5) \quad \begin{aligned} J \left(y_\eta f_\xi^{(p+1)} - y_\xi^{(p+1)} f_\eta \right) &= (y_\eta f_\xi - y_\xi f_\eta) \left(y_\eta x_\xi^{(p+1)} - x_\eta y_\xi^{(p+1)} \right) + O(\Delta\xi)J^2 \\ J \left(f_\xi y_\eta^{(q+1)} - y_\xi f_\eta^{(q+1)} \right) &= (y_\eta f_\xi - y_\xi f_\eta) \left(x_\xi y_\eta^{(q+1)} - y_\xi x_\eta^{(q+1)} \right) + O(\Delta\eta)J^2 \end{aligned}$$

Removing the parentheses and rearranging the corresponding terms Eq.(3.5) can be reduced to

$$(3.6) \quad \begin{aligned} y_\eta \left[f_\xi^{(p+1)} - f_y y_\xi^{(p+1)} - f_x x_\xi^{(p+1)} \right] &= O(\Delta\xi)J \\ y_\xi \left[f_\eta^{(q+1)} - f_y y_\eta^{(q+1)} - f_x x_\eta^{(q+1)} \right] &= O(\Delta\eta)J \end{aligned}$$

Note that a reduction of the $O(\Delta\xi)$ and $O(\Delta\eta)$ terms in Eq.(3.6) decreases the truncation error on the optimal grid.

The above equations can be treated as the optimal grid generation equations in the sense of minimization of the leading truncation error term. It should be noted, that if $y_\xi = 0$ in the entire computational domain Eq.(3.6) is reduced to Eq.(2.14). At the same time, if the y coordinate does not depend on η , i.e. $y = y(\xi)$ Eq.(3.6) is simplified to

$$(3.7) \quad x_\eta f_\eta^{(q+1)} - f_\eta x_\eta^{(q+1)} = O(\Delta\eta)x_\eta^2,$$

that can be treated as an analog of Eq.(2.13) in the η coordinate.

Another very useful property of the optimal mapping is that Eq.(3.6) are invariant with respect to both translation and stretching of the x, y and ξ, η coordinates. Summarizing the above properties of Eq.(3.6) one may conclude that the 2D optimal grid generation equations are fully consistent with the 1D counterpart Eq.(2.14).

The present approach can directly be extended to three dimensions. Actually, the three-dimensional transformation of the first derivative is

$$(3.8) \quad f_x = \frac{z_\zeta y_\eta - y_\zeta z_\eta}{J} f_\xi + \frac{y_\zeta z_\xi - z_\zeta y_\xi}{J} f_\eta + \frac{z_\eta y_\xi - y_\eta z_\xi}{J} f_\zeta$$

where the Jacobian of the mapping is given by

$$J = x_\xi y_\eta z_\zeta + x_\eta y_\zeta z_\xi + x_\zeta y_\xi z_\eta - x_\xi y_\zeta z_\eta - x_\eta y_\xi z_\zeta - x_\zeta y_\eta z_\xi.$$

With p th-, q th-, and r th-order finite difference approximations for the ξ -, η -, and ζ -derivatives, respectively, we have

$$(3.9) \quad L_h(f_x) = \frac{(\delta_\zeta z \delta_\eta y - \delta_\zeta y \delta_\eta z) \delta_\xi f + (\delta_\zeta y \delta_\xi z - \delta_\zeta z \delta_\xi y) \delta_\eta f + (\delta_\eta z \delta_\xi y - \delta_\eta y \delta_\xi z) \delta_\zeta f}{\delta_\xi x \delta_\eta y \delta_\zeta z + \delta_\eta x \delta_\zeta y \delta_\xi z + \delta_\zeta x \delta_\xi y \delta_\eta z - \delta_\xi x \delta_\zeta y \delta_\eta z - \delta_\eta x \delta_\xi y \delta_\zeta z - \delta_\zeta x \delta_\eta y \delta_\xi z} + O(\Delta\xi^{p+1}, \Delta\eta^{q+1}, \Delta\zeta^{r+1}),$$

where the differential operators δ_ξ , δ_η , and δ_ζ are defined by

$$(3.10) \quad \begin{aligned} \delta_\xi &= \frac{\partial}{\partial \xi} + C_p \Delta\xi^p \frac{\partial^{p+1}}{\partial \xi^{p+1}} \\ \delta_\eta &= \frac{\partial}{\partial \eta} + C_q \Delta\eta^q \frac{\partial^{q+1}}{\partial \eta^{q+1}} \\ \delta_\zeta &= \frac{\partial}{\partial \zeta} + C_r \Delta\zeta^r \frac{\partial^{r+1}}{\partial \zeta^{r+1}}. \end{aligned}$$

Here, C_p , C_q , and C_r are constants dependent on particular p th-, q th-, and r th-order finite difference approximations which are applied to discretize the ξ -, η -, and ζ -derivatives, accordingly. In Eq.(3.9),(3.10)

it has already been accounted for that the metric coefficients are approximated by the same finite difference expressions which are used for evaluating f_ξ , f_η , and f_ζ .

Having linearized the fraction in Eq.(3.9) the leading truncation error term is written as

$$(3.11) \quad T_{p,q,r}(\xi, \eta, \zeta) = \frac{1}{J} \left\{ C_p \Delta \xi^p \left[\tilde{F}_\xi^{(p+1)} - \tilde{J}_\xi^{(p+1)} f_x \right] + C_q \Delta \eta^q \left[\tilde{F}_\eta^{(q+1)} - \tilde{J}_\eta^{(q+1)} f_x \right] + C_r \Delta \zeta^r \left[\tilde{F}_\zeta^{(r+1)} - \tilde{J}_\zeta^{(r+1)} f_x \right] \right\},$$

where

$$(3.12) \quad \begin{aligned} \tilde{F}_\xi^{(p+1)} &= f_\xi^{(p+1)} (z_\zeta y_\eta - y_\zeta z_\eta) + y_\xi^{(p+1)} (z_\eta f_\zeta - z_\zeta f_\eta) + z_\xi^{(p+1)} (y_\zeta f_\eta - y_\eta f_\zeta) \\ \tilde{F}_\eta^{(q+1)} &= f_\eta^{(q+1)} (z_\xi y_\zeta - z_\zeta y_\xi) + y_\eta^{(q+1)} (z_\zeta f_\xi - z_\xi f_\zeta) + z_\eta^{(q+1)} (y_\xi f_\zeta - y_\zeta f_\xi) \\ \tilde{F}_\zeta^{(r+1)} &= f_\zeta^{(r+1)} (z_\eta y_\xi - y_\eta z_\xi) + y_\zeta^{(r+1)} (z_\xi f_\eta - z_\eta f_\xi) + z_\zeta^{(r+1)} (y_\eta f_\xi - y_\xi f_\eta) \\ \tilde{J}_\xi^{(p+1)} &= x_\xi^{(p+1)} (z_\zeta y_\eta - y_\zeta z_\eta) + y_\xi^{(p+1)} (z_\eta x_\zeta - z_\zeta x_\eta) + z_\xi^{(p+1)} (y_\zeta x_\eta - y_\eta x_\zeta) \\ \tilde{J}_\eta^{(q+1)} &= x_\eta^{(q+1)} (z_\xi y_\zeta - z_\zeta y_\xi) + y_\eta^{(q+1)} (z_\zeta x_\xi - z_\xi x_\zeta) + z_\eta^{(q+1)} (y_\xi x_\zeta - y_\zeta x_\xi) \\ \tilde{J}_\zeta^{(r+1)} &= x_\zeta^{(r+1)} (z_\eta y_\xi - y_\eta z_\xi) + y_\zeta^{(r+1)} (z_\xi x_\eta - z_\eta x_\xi) + z_\zeta^{(r+1)} (y_\eta x_\xi - y_\xi x_\eta) \end{aligned}$$

Similarly to the 1D and 2D cases described above the leading term of the truncation error Eq.(3.11) can be divided into two parts. The first part, which also exists on a uniform mesh, is due to the approximation of f_ξ , f_η , and f_ζ . The second part, which is vanished on a uniform Cartesian mesh is caused by the evaluation of the metric coefficients. From Eq.(3.11) it is apparent that if a grid is constructed so that the first term in the square brackets is of the order of $O(\Delta\xi)$, the second one is of the order of $O(\Delta\eta)$, and the third one is of the order of $O(\Delta\zeta)$ for all $\xi \in [0, 1]$, $\eta \in [0, 1]$, and $\zeta \in [0, 1]$ then the global order of approximation of the difference operator Eq.(3.9) in ξ , η , and ζ on the optimal grid is increased from p , q , and r to $p+1$, $q+1$, and $r+1$, respectively. Hence, in the sense of minimization of the leading truncation error term the grid adaptation criteria are

$$(3.13) \quad \tilde{F}_\xi^{(p+1)} - f_x \tilde{J}_\xi^{(p+1)} = O(\Delta\xi)J$$

$$(3.14) \quad \tilde{F}_\eta^{(q+1)} - f_x \tilde{J}_\eta^{(q+1)} = O(\Delta\eta)J$$

$$(3.15) \quad \tilde{F}_\zeta^{(r+1)} - f_x \tilde{J}_\zeta^{(r+1)} = O(\Delta\zeta)J.$$

Note that the above equations are not a system of equations and can be considered separately. If it is necessary to improve the accuracy with respect to the ξ coordinate alone a grid should be generated so that only Eq.(3.13) holds. However, if it is desirable to increase the order of approximation of f_x by one in the ξ , η , and ζ coordinates simultaneously then the grid has to obey the system of equations Eq.(3.13)–(3.15).

As in the case of two dimensions the 3D grid adaptation criteria Eq.(3.13)–(3.15) can be simplified. After the substitution of Eq.(3.12) in Eq.(3.13)–(3.15) and considerable algebraic manipulation the grid adaptation equations can be rewritten in a very compact form

$$(3.16) \quad \begin{aligned} (z_\zeta y_\eta - y_\zeta z_\eta) \left[f_\xi^{(p+1)} - f_x x_\xi^{(p+1)} - f_y y_\xi^{(p+1)} - f_z z_\xi^{(p+1)} \right] &= O(\Delta\xi)J \\ (y_\zeta z_\xi - z_\zeta y_\xi) \left[f_\eta^{(q+1)} - f_x x_\eta^{(q+1)} - f_y y_\eta^{(q+1)} - f_z z_\eta^{(q+1)} \right] &= O(\Delta\eta)J \\ (z_\eta y_\xi - y_\eta z_\xi) \left[f_\zeta^{(r+1)} - f_x x_\zeta^{(r+1)} - f_y y_\zeta^{(r+1)} - f_z z_\zeta^{(r+1)} \right] &= O(\Delta\zeta)J, \end{aligned}$$

where f_x , f_y , and f_z are the first derivatives with respect to the x , y , and z coordinates, respectively. One of the characteristic features of the above equations is that they do not depend on the coefficients C_p , C_q , and

C_r . Consequently, if in each spatial direction the metric coefficients and the first derivatives of $f(\xi, \eta, \zeta)$ are evaluated consistently by some hybrid finite difference operators then the grid adaptation criteria Eq.(3.16) can be applied in the whole computational domain regardless of points where the hybrid scheme switches from one approximation to another. A comparison of Eq.(3.16), Eq.(3.6), and Eq.(2.13) shows that the 3D grid adaptation criteria Eq.(3.16) are reduced to Eq.(3.6) if $z_\xi = z_\eta = 0, z_\zeta \neq 0$, while if in addition to these conditions we require that $y_\xi = y_\zeta = 0, y_\eta \neq 0$ Eq.(3.16) are reduced to the 1D optimal grid generation equation Eq.(2.13). In a similar manner as Eq.(2.13) and Eq.(3.6), it is easy to prove that Eq.(3.16) are invariant with respect to stretching and translation of both the physical and computational coordinates.

As it follows from the analysis presented in the foregoing section the grid adaptation equation does not assure that the coordinate mapping obtained as the solution of Eq.(2.14) is not singular. Since Eq.(3.16) is converted to Eq.(3.6) and in its turn Eq.(3.6) is reduced to Eq.(2.14) if the dimension of the space is decreased by one, the same singularity may occur in two and three dimensions as well.

Equations (3.6) and (3.16) have to be closed by corresponding boundary conditions. Since these equations are $(p+1)$ th-order partial differential equations $p+1$ boundary conditions should be imposed at each couple of the opposite boundaries (i.e. $\xi = 0$ and $\xi = 1$; $\eta = 0$ and $\eta = 1$; $\zeta = 0$ and $\zeta = 1$) to find the unique solution. However, at each boundary we have only one boundary condition. For example, in the 3D case in the ξ coordinate we have

$$(3.17) \quad \xi(x, y, z) = 0, \quad \xi(x, y, z) = 1.$$

In other words Eq.(3.6) and Eq.(3.16) are not closed. The situation becomes even more uncertain when only one of the grid adaptation criteria is used. However, this uncertainty gives us additional degrees of freedom and at the same time, it is conceivable that there exists more than one optimal grid satisfying the criteria Eq.(3.6) or Eq.(3.16). From this standpoint both Eq.(3.6) and Eq.(3.16) should be treated as the grid adaptation criteria rather than the optimal grid generation equations.

One of the most general structured grid generation strategies is based on the variational approach proposed by Brackbill and Saltzman in [17]. In this method a grid is generated as the solution of the minimization problem. By forming the variational principle using a linear combination of the integral measures of smoothness, orthogonality, and adaptation, a system of elliptic equations is derived. The new grid adaptation criteria can be incorporated into this approach by constructing an integral measure of adaptation so that the Euler-Lagrange equations associated with the minimization of this integral alone give us Eq.(3.16). On the one hand, the minimax principle guarantees that the coordinate mapping obtained as the solution of this minimization problem is not singular. On the other hand, the new grid adaptation criteria provide that the leading term of the truncation error is minimized so that the finite difference approximation Eq.(3.9) calculated on the optimal grid exhibits superconvergence properties.

Remark 3.1 In spite on the fact that the present analysis has been performed for the first derivative f_x it can be directly extended to an equation or a system of equations, which can be represented as

$$(3.18) \quad f_x(x) = d(x).$$

For example, for the steady state 1D Burgers equation written in conservation law form we have

$$(3.19) \quad \frac{\partial}{\partial x} \left(\frac{u^2}{2} - \mu \frac{\partial u}{\partial x} \right) = 0,$$

where μ is a positive constant. A comparison of Eq.(3.19) and f_x shows that for the Burgers equation the

optimal grid can be constructed using Eq.(2.54) with

$$(3.20) \quad f(x) = \frac{u^2}{2} - \mu \frac{\partial u}{\partial x}.$$

It should be pointed out that the above conclusion is valid if the second derivative $u_{xx} = (u_x)_x$ and the convective term $(u^2/2)_x$ are approximated consistently.

The same approach can be applied to the Euler and Navier-Stokes equations. The 1D Euler and Navier-Stokes equations can be written in conservation law form as

$$(3.21) \quad \frac{\partial \mathbf{F}}{\partial x} = 0,$$

where \mathbf{F} is the inviscid flux \mathbf{F}_i for the Euler equations and $\mathbf{F}_i - \mathbf{F}_v$, where \mathbf{F}_v is the viscous flux, for the Navier-Stokes equations. As it follows from Eq.(3.16), any component of the vector \mathbf{F} can be chosen as a function with respect of which a grid is adapted. Although, that choice provides increase in accuracy for this particular vector component but it may not result in decrease in the truncation error for the remaining vector components. In fact, as there are components of the vector \mathbf{F} as many the optimal grids can be generated. Since the different vector components may have strong gradients and local extrema in different regions of the physical domain this kind of grid adaptation is not effective. If this is the case the function $f(x)$ can be obtained by using the method of least squares. Because of the optimal grid generation equations are invariant with respect to stretching of the function $f(x)$ the vector components F_n , $n = \overline{1, N}$ can be normalized as

$$(3.22) \quad \tilde{F}_n(x) = \frac{|F_n(x)|}{\max_x |F_n(x)|}.$$

It results in that all of the vector components are of the same order and, consequently, make proportional contributions to the function $f(x)$. The resulting function $f(x)$ is obtained as the solution of the following minimization problem

$$(3.23) \quad \sum_{i=0}^I \sum_{n=1}^N \left(\tilde{F}_n(x_i) - f(x_i) \right)^2 \rightarrow \min$$

in the least square sense. The function f constructed in this fashion allows one to generate a grid which is optimal for the whole vector \mathbf{F} rather than for its particular component. Note that the power in Eq.(3.23) should be chosen in accordance with the power of the L_k norm in which the solution of the Euler or Navier-Stokes equations is sought.

4. Results and Discussion. To validate the applicability and efficiency of the new method several 1D and one 2D test examples are considered. For each 1D test function five series of calculation on different grids with the same number of grid points have been executed. The first one is done on a uniform grid. The second one uses the standard grid adaptation criterion based on the arc length or the second derivative of the test function. The third one is performed on the optimal grid obtained as the analytical solution of Eq.(2.14). The fourth one employs the optimal grid Eq.(2.54) generated numerically by using the following approximation for the second derivative

$$(4.1) \quad (f_{xx})_i = \frac{h_i f_{i+1} - (h_i + h_{i+1}) f_i + h_{i+1} f_{i-1}}{h_i h_{i+1} (h_i + h_{i+1}) / 2}, \quad h_i = x_i - x_{i-1},$$

which is reduced to the second-order three-point central approximation of f_{xx} if an equispaced grid in the physical domain is used. The integrals in Eq.(2.54) is computed using the trapezoidal rule integration. As

a result of this integration the strictly increasing function $\xi(x)$ is obtained which is then reversed by using a third-order accurate piecewise spline interpolation. The fifth calculation is also executed on the uniform grid, however, instead of a p th-order approximation a $(p + 1)$ th-order accurate discretization is applied to calculate both f_ξ and x_ξ . At each boundary one-sided p th-order differences are used for f_ξ and x_ξ .

In order to estimate the accuracy of the method the p th-order finite difference approximation of f_x is compared with the exact value of the first derivative calculated at the same grid node in the L_2 norm. The order of approximation is estimated on successively refined grids the coarsest one of which contains 20 cells and the finest one has 2560 cells.

4.1. 1D Test Examples. Second-order approximation, $p = 2$

The first test example is evaluation of the first derivative of $f(x) = x^m$, $0 \leq x \leq 1$ by using a second-order central differences for f_ξ and x_ξ . When m is sufficiently large this function has a boundary layer of width $O(1/m)$ near $x = 1$. For this test case the exact optimal grid point distribution defined by Eq.(2.21) can be found analytically, which is

$$(4.2) \quad x_{opt}(\xi) = \xi^{\frac{3}{m+1}}.$$

In contrast to [9] the new grid adaptation criterion provides the concentration of grid nodes near the boundary layer of the function $f(x)$.

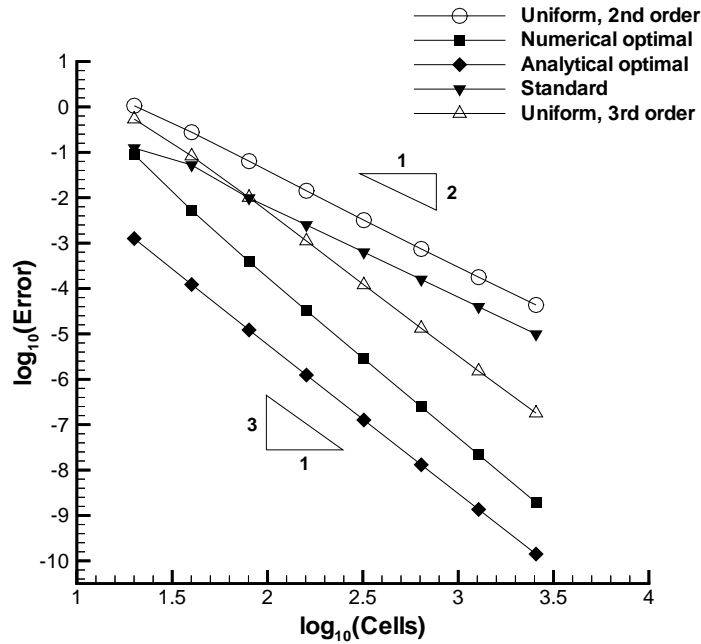


FIG. 4.1. Error convergence for a second-order approximation of f_x , $f(x) = x^m$ calculated on: 1) uniform grid, 2) optimal grid generated numerically, 3) analytical optimal grid, 4) grid adapted in accordance with the arc length criterion, 5) uniform grid using third-order accurate discretization.

An error convergence plot for this test function is presented in Fig.4.1. As one might expect, the L_2 norm of the truncation error calculated on a uniform grid exhibits the $O(\Delta\xi^2)$ convergence rate which is consistent with the second order of accuracy of the central differences. However, the same second-order approximation of f_x on the optimal grid Eq.(4.2) exhibits the convergence rate which is even higher than

$O(\Delta\xi^3)$. Although, the accuracy of f_x obtained on the adaptive grid Eq.(2.26) with f_{xx} evaluated by Eq.(4.1) is slightly less compared to the optimal grid Eq.(4.2) results the order of approximation is about 3.5. To show the superiority of the present method over the standard grid adaptation criterion Eq.(2.41) the truncation error calculated on grids adapted in accordance with the arc length of $f(x)$ is also shown in Fig.4.1. In spite of the fact that the standard grid adaptation technique slightly improves the accuracy of calculation in comparison with the equispaced grid point distribution the convergence rate is less than $O(\Delta\xi^2)$. We want to emphasize that the new grid adaptation criterion Eq.(2.26) provides not only superconvergent results, but on the finest mesh it reduces the error by 6 orders of magnitude compared to the uniform grid results.

An advantage of the consistent grid adaptation Eq.(2.14), which is based on the fact that the truncation errors due to the approximation of f_ξ and x_ξ cancel each other, becomes obvious when the optimal grid results are compared with those obtained by using a third-order accurate approximation on a uniform grid. Figure 4.1 shows that both the second-order approximation on the optimal grid and the third-order discretization on the uniform grid with the same number of grid points reveal the $O(\Delta\xi^3)$ convergence rate. However, the optimal grid results are about 10^3 times more accurate.

It should be noted that the optimal grid Eq.(4.2) is essentially non-smooth and does not meet the standard criterion of smoothness, which is $|x_{\xi\xi}/x_\xi| < O(1)$ [18]. Furthermore, the optimal mapping Eq.(4.2) is singular at the point $\xi = 0$ where $x_\xi \rightarrow \infty$. In spite on this fact, the above comparisons corroborate the theoretical analysis and demonstrate the advantage of the new grid adaptation criterion over the standard approaches.

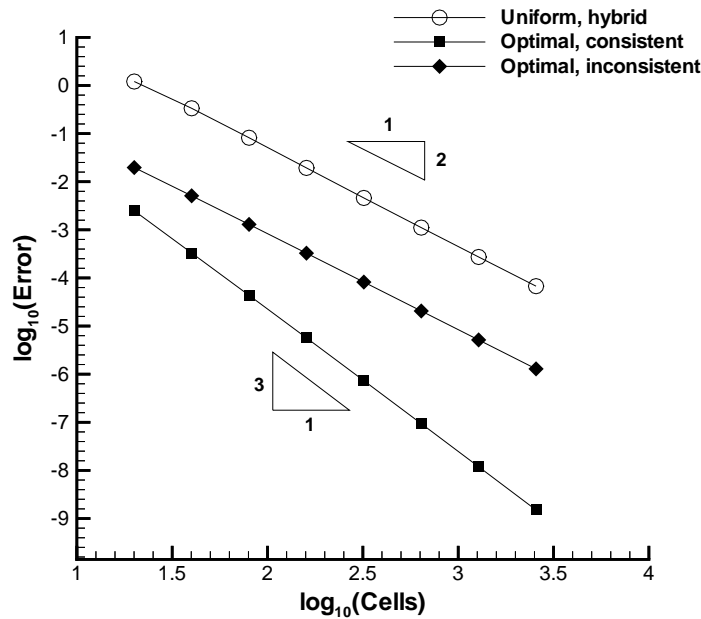


FIG. 4.2. Error convergence of a second-order hybrid approximation calculated with the consistent and inconsistent discretizations of the metric coefficient on the optimal and uniform grids.

Another very useful characteristic feature of the new method is its generality in the sense that if a single second-order hybrid discretization is used for both f_ξ and x_ξ the same optimal mapping Eq.(4.2) minimizes the leading truncation error term. To demonstrate this property the error convergence of the

hybrid approximation obtained on the uniform and optimal grids with the same number of grid points are depicted in Fig.4.2. The hybrid difference operator is constructed as follows

$$(4.3) \quad \left(\frac{\partial f}{\partial \xi}\right)_i = \begin{cases} \frac{1}{2\Delta\xi}(f_{i+1} - f_{i-1}), & i \text{ even} \\ \frac{1}{2\Delta\xi}(-3f_i + 4f_{i+1} - f_{i+2}), & i \text{ odd} \end{cases}$$

The identical approximation is employed for the metric coefficient x_ξ . A comparison shows that the global order of the consistent approximation of f_ξ and x_ξ is increased by one on the same optimal grid Eq.(4.2) used for the non-hybrid approximation. As has been shown in Section 2, the approximation of the metric coefficient and the first derivative f_ξ should be the same otherwise the optimal mapping defined by Eq.(2.26) does not minimize the leading truncation error term. To show that the discretization of the metric coefficient plays a crucial role in reduction of the truncation error we approximate x_ξ by a two-point central difference expression in the whole computational domain and use the same hybrid scheme Eq.(4.3) for f_ξ . An error convergence plot for this inconsistent approximation, which is also depicted in Fig.4.2, shows that if the metric coefficient are evaluated in a different way than f_ξ the order of approximation on the optimal grid deteriorates to 2 as well as the truncation error increases by a factor of 10^3 compared to the consistent discretization results.

The second test function considered is

$$(4.4) \quad f(x) = \frac{1}{(e^m - 1)x + 1}, \quad 0 \leq x \leq 1.$$

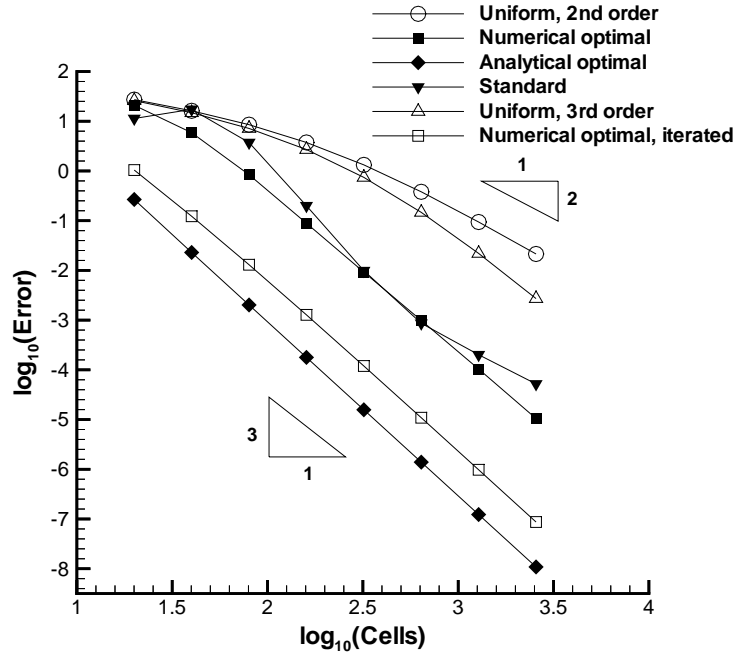


FIG. 4.3. Error convergence for a second-order approximation of f_x , $f(x) = 1/((e^m - 1)x + 1)$ calculated on: 1) uniform grid, 2) optimal grid generated numerically, 3) analytical optimal grid, 4) grid adapted in accordance with the arc length criterion, 5) uniform grid using third-order accurate discretization, 6) numerical optimal grid generated iteratively.

In the present test example the parameter m was chosen to be 5. This function has a boundary layer of width $O(m/(e^m - 1))$ at $x = 0$. For this function the optimal grid generation equation Eq.(2.14), which

depends on the order of approximation rather than on a particular type of discretization, can be solved analytically, that gives

$$(4.5) \quad x_{opt}(\xi) = \frac{e^{m\xi} - 1}{e^m - 1}.$$

It should be emphasized that Eq.(2.26) yields the same optimal mapping as Eq.(4.5). The optimal grid Eq.(4.5) is the well-known exponential coordinate transformation, which is widely used in the literature [1], [18] for solving boundary layer problems. However, the mapping Eq.(4.5) is optimal only for a special class of functions such as Eq.(4.4) and not optimal for other functions. Similarly to Fig.4.1 and 4.2, error convergence plots for the symmetric second-order and hybrid discretizations Eq.(4.3) are depicted in Fig.4.3 and 4.4, respectively. It is apparent in these figures that the error obtained on the optimal grid reveals the convergence rate of $O(\Delta\xi^{3.5})$ that is even higher than it follows from the theoretical analysis. The optimal grid point distribution constructed by the numerical integration of Eq.(2.26) reduces the truncation error by about four orders of magnitude compared to the uniform grid results, but it does not provide the same accuracy as the optimal grid Eq.(4.5). The accuracy can be improved if the following iterative procedure is applied. Since the f_{xx} approximation Eq.(4.1) depends on the grid spacing in the physical domain, the second derivative can be updated when the new grid point distribution is found. For this test problem about 15–20 iterations were needed to reach the convergence. No attempt was made to optimize the iteration process. Referring to Fig.4.3 one can see that this procedure considerably increases the accuracy and provides practically the same convergence rate as for the analytical optimal grid Eq.(4.5).

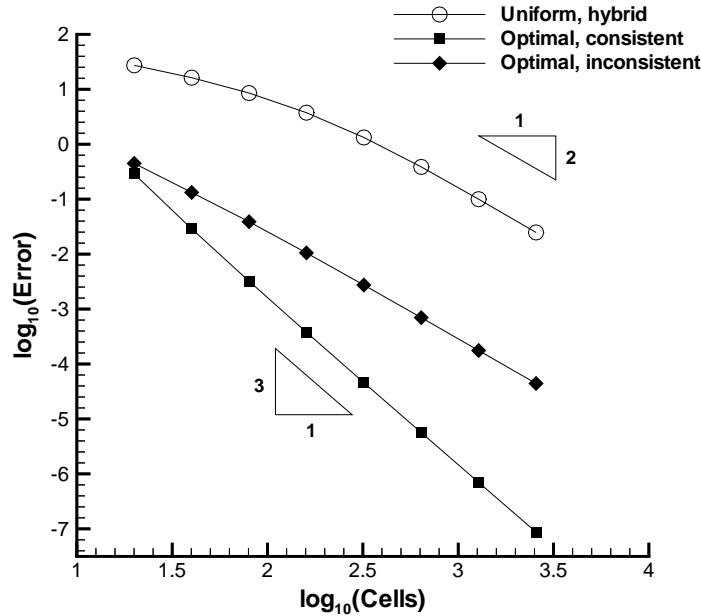


FIG. 4.4. Error convergence of a second-order hybrid approximation calculated with the consistent and inconsistent discretizations of the metric coefficient on the optimal and uniform grids.

The importance of the metric coefficient evaluation is illustrated in Fig.4.4. Analogously to the foregoing test case, the inconsistent discretization of f_ξ and x_ξ leads to decrease in both the order and accuracy of the approximation. When the metric coefficient and the first derivative f_ξ are evaluated by using the same

hybrid operator Eq.(4.3) the convergence rate obtained on the optimal grid Eq.(4.5) becomes $O(\Delta\xi^3)$.

From the present theoretical analysis it follows that the new grid adaptation strategy may be quite sensitive to the inflection points of the function $f(x)$. In order to verify this conclusion the following function

$$(4.6) \quad f(x) = \frac{1}{36m^2} [\sin(3mx) - 27\sin(mx)], \quad 0 \leq x \leq \pi,$$

which has m inflection points has been chosen as a test function. Despite the presence of the inflection points where $f_{xx} = 0$ it is possible to construct the optimal mapping analytically without using Eq.(2.30). It can be done if the optimal grid Eq(2.26) is generated in each interval of constant signs of f_{xx} separately. Thus, we have

$$(4.7) \quad x_{opt}(\xi) = \frac{\pi}{m}(j-1) + \frac{1}{m} \arccos[2j - 2m\xi - 1], \quad \frac{j-1}{m} \leq \xi \leq \frac{j}{m}, \quad j = \overline{1, m}.$$

In numerical calculations the parameter m was taken to be 5. The above optimal coordinate transformation obeys Eq.(2.26) in the entire physical domain except for the inflection points.

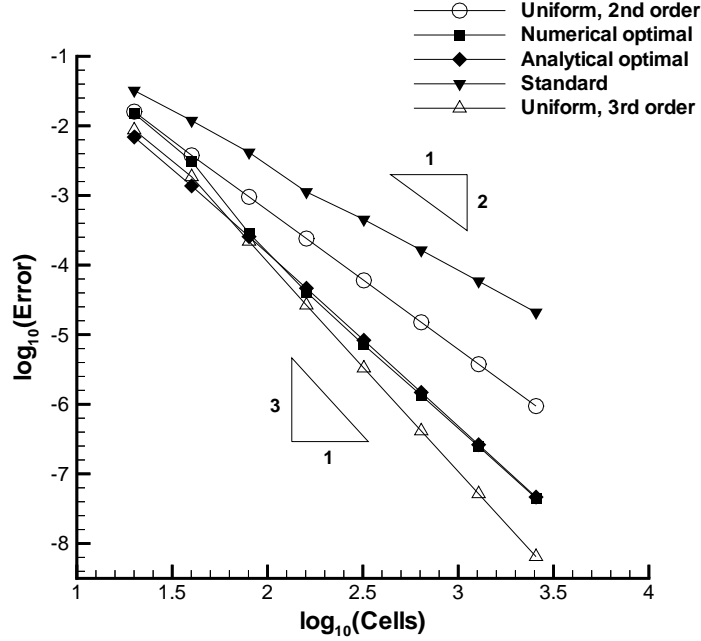


FIG. 4.5. Error convergence for a second-order approximation of f_x , calculated on: 1) uniform grid, 2) optimal grid generated numerically, 3) analytical optimal grid, 4) grid adapted in accordance with the arc length criterion, 5) uniform grid using third-order accurate discretization.

Figures 4.5 and 4.6 are analogous to Fig.4.1 and 4.2, accordingly. As one can see in Fig.4.5 the presence of the inflection points results in that the convergence rate is $O(\Delta\xi^{2.5})$ that is lower than it is predicted from the theoretical analysis. Nevertheless, the optimal grid adaptation reduces the truncation error by a factor of 20 compared to the uniform grid results. One of the reasons of such a behavior is the fact that high-order derivatives of the function $f(x)$ Eq.(4.6) are well bounded that makes the approximation of f_x on the uniform grid sufficiently accurate. The use of the standard grid adaptation criterion based on \tilde{f}_{xx} Eq.(2.30) leads to deterioration of the convergence rate to $O(\Delta\xi^{1.5})$ and at the same time, the L_2 norm of the truncation error is about 50 times less accurate than the uniform grid results. Figure 4.6 shows that the

inconsistent approximation of f_ξ and x_ξ increases the truncation error by 5 orders of magnitude compared to the consistent approximation results calculated on the optimal grid.

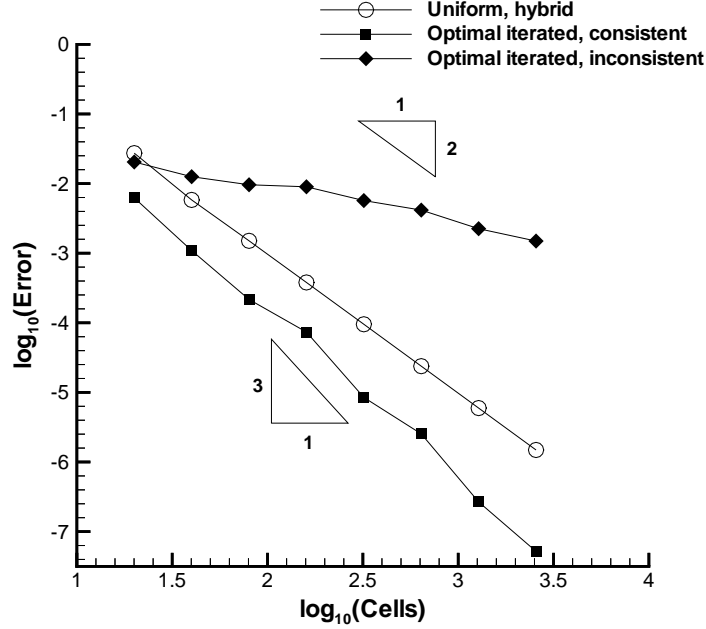


FIG. 4.6. Error convergence of a second-order hybrid approximation calculated with the consistent and inconsistent discretizations of the metric coefficient on the optimal and uniform grids.

To gain greater insight into where the maximum error occurs pointwise error distributions obtained on both the uniform and optimal grids are shown in Fig.4.7. As expected, the truncation error calculated on the optimal grid achieves its maximum values at the inflection points, while the error on the uniform grid occurs at points where the third derivative $|f_{xxx}|$ is large. In contrast to the uniform grid, the most accurate approximation of the first derivative f_x on the optimal grid is near the local extrema of $f(x)$. For demonstrating the gain in accuracy in the vicinity of the inflection points due to the use of Eq.(2.30) instead of f_{xx} a pointwise error plot obtained in this case is also presented in Fig.4.7. It is significant that the error distribution obtained on the optimal grid is essentially nonuniform that gives an indication of the difference between the present and equidistribution grid adaptation criteria.

From the practical point of view it is very important to improve the accuracy of calculation if the function $f(x)$ is discontinuous. In spite of the fact that the present analysis is not valid at discontinuities of $f(x)$ it can be used if the discontinuous function is approximated by some smooth one. In this test example the following smooth function

$$(4.8) \quad f(x) = \frac{2\epsilon x [17 + 73(\epsilon x)^2 + 55(\epsilon x)^4 + 15(\epsilon x)^6]}{15\pi(1 + (\epsilon x)^2)^4} + \frac{2}{\pi} \arctan(\epsilon x), \quad -1 \leq x \leq 1$$

is considered as a fitting of a step function. In this calculation the parameter ϵ was taken to be 10^3 that results in that the function Eq.(4.8) has a pronounced interior layer of width $O(1/\epsilon)$ at $x = 0$. This function has been chosen so that the optimal grid point distribution Eq.(2.26) can be integrated analytically. As in the foregoing example, the singularity in the optimal mapping Eq.(2.26) due to the inflection point at $x = 0$ can be overcome by generating the optimal grid in the $-0.5 \leq x < 0$ and $0 \leq x \leq 0.5$ intervals separately,

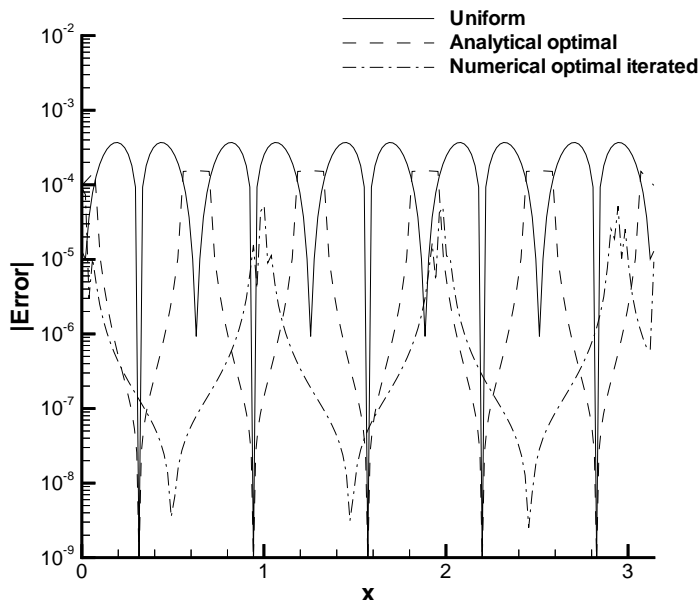


FIG. 4.7. Pointwise error distribution for a second-order approximation calculated on the analytical optimal, numerical optimal, and corresponding uniform grids.

that gives

$$(4.9) \quad x_{opt}(\xi) = \begin{cases} -\sqrt{\frac{1-2\xi}{1+2\varepsilon^2\xi}}, & 0 \leq \xi < 0.5 \\ \sqrt{\frac{2\xi-1}{1+2\varepsilon^2(1-\xi)}}, & 0.5 \leq \xi \leq 1. \end{cases}$$

The error convergence of the symmetric second-order discretization of f_x evaluated on the optimal grid Eq.(4.9) is compared with results obtained by second- and third-order approximations on a uniform grid as well as with the truncation error calculated on grids generated by using the standard Eq.(2.41) and new Eq.(2.26),(2.30) grid adaptation criteria in Fig.4.8. Because of the internal layer thickness is comparable with the finest grid spacing none of the uniform grids considered can provide second-order results. For the analytical optimal grid the convergence rate is of the order of $O(\Delta\xi^{2.5})$. Although, it is less than the theoretical limit the truncation error on the finest mesh (2560 cells) has been reduced by more than 5 orders of magnitude compared to the uniform grid results. Since the standard grid adaptation criterion Eq.(2.41), which is widely used to improve the resolution near steep gradients of the solution, does not provide the cancellation of the leading truncation error term these results are about 2 orders of magnitude less accurate than those obtained on the optimal grid Eq.(2.26),(4.1),(2.30) as is evident in Fig.4.8.

A comparison of the hybrid approximation Eq.(4.3) on different grids and using different approximations for the metric coefficient x_ξ is presented in Fig.4.9. If f_ξ and x_ξ are evaluated identically the same optimal grid Eq.(4.9) provides superconvergent results, while if these approximations are different the convergence rate is even less than $O(\Delta\xi^2)$.

High-order approximations, $p \geq 3$

For a third-order discretization the optimal grid generation equation Eq.(2.51) can not be solved analytically, however, the solution can be found in the approximate form of Eq.(2.53),(2.54). The same function

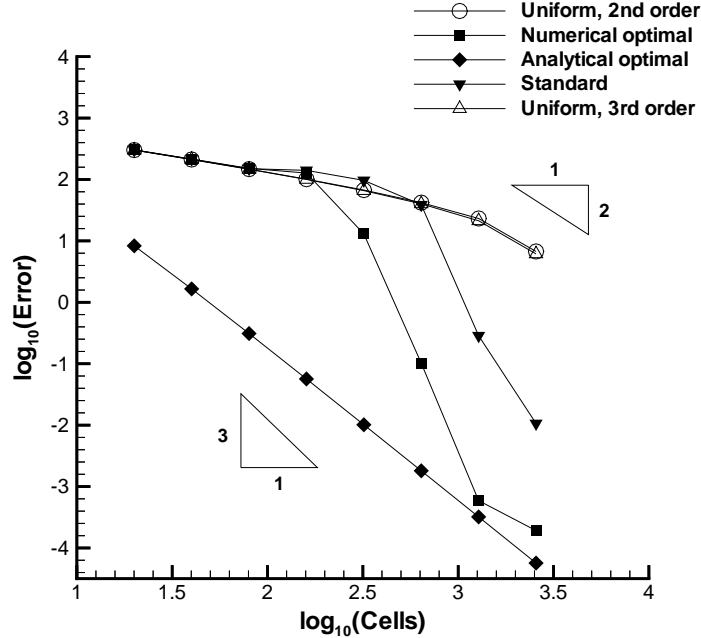


FIG. 4.8. Error convergence for a second-order approximation of f_x , calculated on: 1) uniform grid, 2) optimal grid generated numerically, 3) analytical optimal grid, 4) grid adapted in accordance with the arc length criterion, 5) uniform grid using third-order accurate discretization.

Eq.(4.4), which has been used in the second example is taken as a test function. The first derivative f_ξ and the metric coefficient are evaluated by a third-order accurate formula as

$$(4.10) \quad (g_\xi)_i = \frac{1}{6\Delta\xi} (-2g_{i-1} - 3g_i + 6g_{i+1} - g_{i+2}),$$

where $g(\xi)$ is either $f(\xi)$ or $x(\xi)$.

Figure 4.10 shows error convergence plots obtained on the optimal Eq.(2.53),(2.54) and uniform grids with the same number of grid cells. Although, for the mapping Eq.(2.53),(2.54) the leading term of the truncation error is approximately equal to zero the error convergence rate obtained on the optimal grid is about $O(\Delta\xi^{3.8})$ that corroborates the theoretical results. Note that the same iterative technique used earlier for the second-order approximations can be applied in the present case as well. However, due to the fact that the optimal coordinate transformation Eq.(2.53),(2.54) is the approximate solution of Eq.(2.51) the iterations do not practically improve the accuracy of calculation and therefore, these results are not presented here.

The truncation error can be reduced if the optimal grid generation equation Eq.(2.48) is solved numerically. To avoid the solution of the third-order differential equation a new dependent variable $u(x) = \xi_x$ is introduced. Then Eq.(2.48), which is a second-order differential equation in terms of $u(x)$, is integrated numerically on a uniform grid constructed in the physical domain. To close Eq.(2.48) the metric coefficient ξ_x is taken to be proportional to $(\tilde{f}_{xx})^{1/4}$ at the boundaries. The metric coefficient ξ_x found this way is integrated and the optimal grid point distribution is obtained by a third-order accurate piecewise spline interpolation of the function $\xi(x)$. As one can see in Fig.4.10, these optimal grid results exhibit the convergence rate of essentially $O(\Delta\xi^4)$ and provide higher accuracy than those calculated on the optimal grid Eq.(2.53),(2.54).

To demonstrate the superiority of the optimal grid adaptation over the equispaced grid point distribution an error convergence plot of a symmetric fourth-order accurate approximation of f_x calculated on a uniform

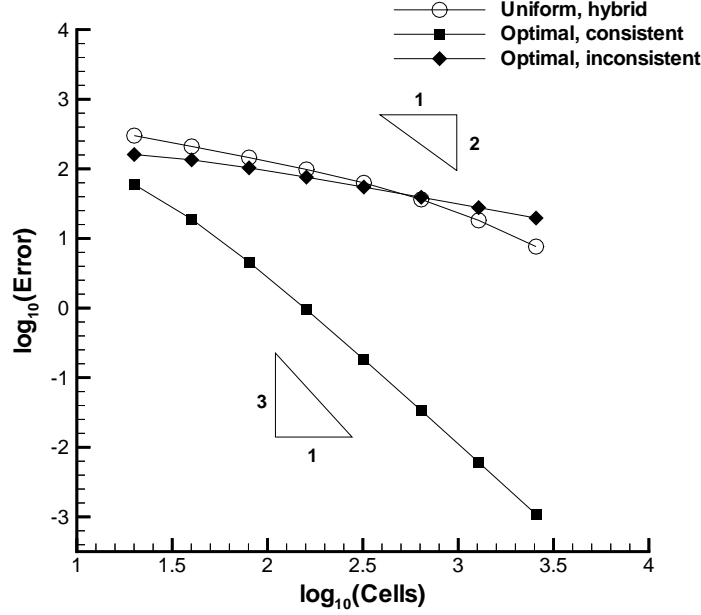


FIG. 4.9. Error convergence of a second-order hybrid approximation calculated with the consistent and inconsistent discretizations of the metric coefficient on the optimal and uniform grids.

grid with the same number of grid points is also depicted in Fig.4.10. The L_2 norm of the truncation error of the third-order approximation Eq.(4.10) on the optimal grid is reduced by a factor of several hundred in comparison with the fourth-order accurate results obtained on the uniform grid.

Error convergence plots for the following hybrid approximation

$$(4.11) \quad \left(\frac{\partial f}{\partial \xi}\right)_i = \begin{cases} \frac{1}{6\Delta\xi} (-2f_{i-1} - 3f_i + 6f_{i+1} - f_{i+2}), & i \text{ even} \\ \frac{1}{6\Delta\xi} (-11f_i + 18f_{i+1} - 9f_{i+2} + 2f_{i+3}), & i \text{ odd} \end{cases}$$

calculated on the optimal and corresponding uniform grids are shown in Fig.4.11. The optimal grid results are about 4–5 orders of magnitude more accurate than those obtained on the finest uniform grid. However, if the metric coefficient is evaluated by Eq.(4.10) in the entire computational domain while the approximation of f_ξ remains the same Eq.(4.11) the error convergence rate of this inconsistent discretization becomes even less than $O(\Delta\xi^3)$ as the grid is refined.

The next test example is a fourth-order accurate approximation of the first derivative of the function $f(x) = x^m$, where the parameter m has been chosen to be 49. The first derivatives f_ξ and x_ξ are discretized by a five-point symmetric approximation

$$(4.12) \quad (g_\xi)_i = \frac{1}{12\Delta\xi} (g_{i-2} - 8g_{i-1} + 8g_{i+1} - g_{i+2}),$$

where $g(\xi)$ is either $f(\xi)$ or $x(\xi)$. It can be shown that if the order of approximation p is an even number then for $f(x) = x^m$ the optimal grid generation equation Eq.(2.14) can be solved analytically. Thus, we have

$$(4.13) \quad x_{opt}(\xi) = \xi^{\frac{p+1}{m+1}}.$$

The above mapping is optimal in the sense of the minimization of the leading truncation error term if $m > p$ otherwise any p th-order accurate difference expression approximates the first derivative f_x exactly. If we fix

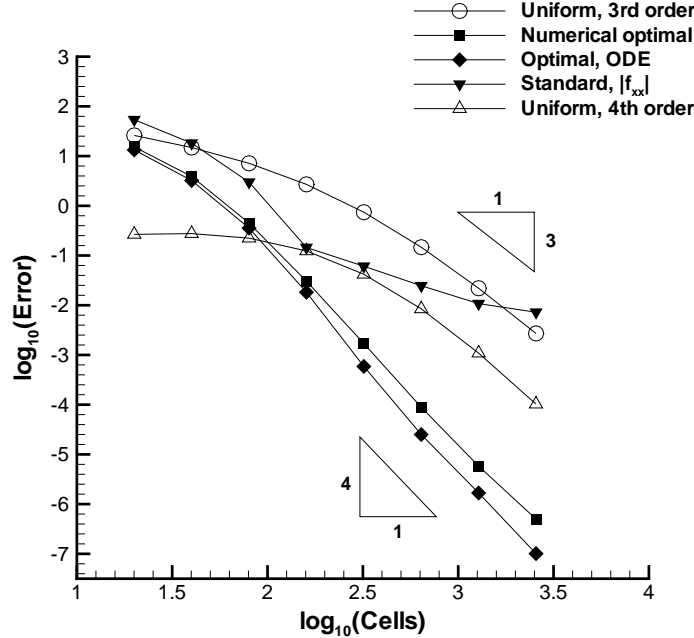


FIG. 4.10. Error convergence for a third-order approximation of f_x , $f(x) = x^m$ calculated on: 1) uniform grid, 2) optimal grid generated numerically, 3) analytical optimal grid, 4) grid adapted in accordance with the arc length criterion, 5) uniform grid using fourth-order accurate discretization.

the parameter m to be sufficiently large one can observe that as the order of approximation p is increased the optimal grid Eq.(4.13) becomes more uniform that correlates with the above theoretical analysis. The optimal grid point distribution can also be calculated numerically by using Eq.(2.54). At each grid point the unknown parameter $\alpha(x)$ is found as a solution of the equation

$$(4.14) \quad T_4(\alpha) = 0,$$

where $T_4(\alpha)$ is given by Eq.(2.59). For this particular choice of the function $f(x)$, Eq.(4.14) can be solved analytically that yields

$$(4.15) \quad \alpha = \frac{1}{5} \frac{m-4}{m-2}.$$

Note that the optimal mapping Eq.(2.54),(4.15) is identical to Eq.(4.13) if we set $p = 4$ in it. Error convergence plots calculated on the analytical Eq.(4.13) and numerical Eq.(2.54),(4.15) optimal grids as well as on the corresponding uniform grid are shown in Fig.4.12. As one can see in this figure the fourth-order approximation Eq.(4.12) on the optimal grid Eq.(4.13) exhibits even a higher convergence rate than $O(\Delta\xi^5)$ that allows one to reduce the L_2 norm of the truncation error by 6 orders of magnitude compared to the uniform grid results. The numerical approximation of both the second derivative and the integral in Eq.(2.54) leads to that the optimal grid Eq.(2.54),(4.15) generated numerically provides superconvergent results only on coarse grids while as the grid is refined the order of approximation deteriorates to 4. Nevertheless, the evaluation of f_x on the 80-cell optimal grid Eq.(2.54),(4.15) is about 3 orders of magnitude more accurate than that on the uniform grid with the same number of grid points. One of the main reasons of such a behavior is an error introduced by the numerical approximation of f_{xx} in Eq.(2.54). As mentioned above, the optimal mapping Eq.(4.13) is singular at $\xi = 0$ that considerably decreases the accuracy of the f_{xx}

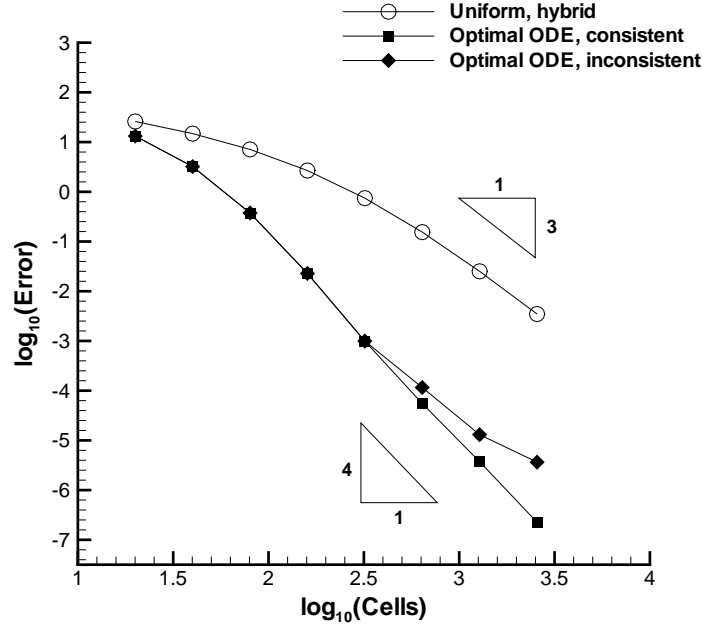


FIG. 4.11. Error convergence of a third-order hybrid approximation calculated with the consistent and inconsistent discretizations of the metric coefficient on the optimal and uniform grids.

approximation Eq.(4.1). This perturbation introduced into the optimal grid by the numerical evaluation Eq.(4.1) destroys the superconvergence property. However, if one uses the exact expression for f_{xx} despite that the integral in Eq.(2.54) and $x(\xi)$ are calculated numerically, the order of approximation is practically recovered to its optimal value that can be seen in Fig.4.12.

To demonstrate the importance of the consistent approximation of f_ξ and x_ξ error convergence plots calculated using different hybrid approximations on the optimal and corresponding uniform grids are depicted in Fig.4.13. The fourth-order accurate hybrid approximation is constructed as follows

$$(4.16) \quad (f_\xi)_i = \begin{cases} \frac{1}{12\Delta\xi} (f_{i-2} - 8f_{i-1} + 8f_{i+1} - f_{i+2}), & i \text{ even} \\ \frac{1}{12\Delta\xi} (-3f_{i-1} - 10f_i + 18f_{i+1} - 6f_{i+2} + f_{i+3}), & i \text{ odd} \end{cases}$$

If the metric coefficient x_ξ is evaluated by the same difference expression employed for the first derivative f_ξ Eq.(4.16) then the leading term of the truncation error is vanished on the optimal grid Eq.(4.13). It is evident in Fig.4.13 that the truncation error of the consistent hybrid approximation of f_ξ and x_ξ exhibits the convergence rate of $O(\Delta\xi^5)$. At the same time, if the metric coefficient is discretized by the symmetric fourth-order accurate formula Eq.(4.12) in the entire computational domain, while the same approximation Eq.(4.16) is used for f_ξ , the convergence rate deteriorates to $O(\Delta\xi^4)$ and the truncation error increases by a factor of 50–100 in comparison with the consistent approximation results. The deterioration of the error convergence rate on the finest optimal mesh is presumably caused by the machine accuracy.

4.2. 2D Test Example. We shall seek a particular solution of Eq.(3.6) in the following form

$$(4.17) \quad \begin{aligned} f(\xi, \eta) &= e^{\alpha\xi} e^{\beta\eta} \\ x_{opt}(\xi, \eta) &= e^{\gamma\xi} e^{\phi\eta} \\ y_{opt}(\xi, \eta) &= e^{\theta\xi} e^{\psi\eta}, \end{aligned}$$

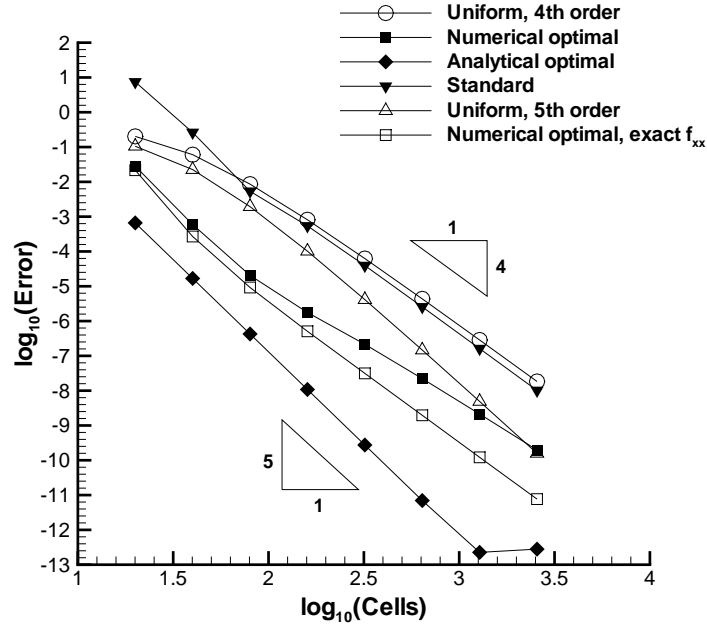


FIG. 4.12. Error convergence for a fourth-order approximation of f_x , $f(x) = x^m$ calculated on: 1) uniform grid, 2) optimal grid generated numerically, 3) analytical optimal grid, 4) grid adapted in accordance with the arc length criterion, 5) uniform grid using fifth-order accurate discretization, 6) numerical optimal grid generated with the exact f_{xx} .

where α , β , and γ , ϕ , θ , ψ are given and unknown constants, respectively. Note that this choice of f , x , and y uniquely defines the function $f(x, y)$ in the physical domain. Since the above mapping must be nonsingular the Jacobian of the mapping, which is

$$(4.18) \quad J(\xi, \eta) = (\gamma\psi - \phi\theta)e^{(\gamma+\theta)\xi}e^{(\phi+\psi)\eta},$$

should be positive in the whole computational domain that leads to

$$(4.19) \quad \gamma\psi - \phi\theta > 0.$$

Substituting Eq.(4.17) into the first equation of Eq.(3.6) yields

$$(4.20) \quad (\gamma\psi - \phi\theta)\alpha^3 = (-\phi\alpha + \gamma\beta)\theta^3 + (\psi\alpha - \theta\beta)\gamma^3.$$

Equation (4.20) together with the constraint Eq.(4.19) give us a family of the optimal grids. The equation is simplified considerably if we assume that $\phi = \psi = \beta = 1$. Under this assumption Eq.(4.20) and (4.19) are reduced to

$$(4.21) \quad (\gamma - \theta)\alpha^3 = (\gamma - \alpha)\theta^3 + (\alpha - \theta)\gamma^3$$

$$(4.22) \quad \gamma - \theta > 0,$$

correspondingly. Equation (4.21) has three real roots

$$(4.23) \quad \begin{aligned} \gamma_1 &= \alpha - \theta \\ \gamma_2 &= \theta \\ \gamma_3 &= \alpha \end{aligned}$$

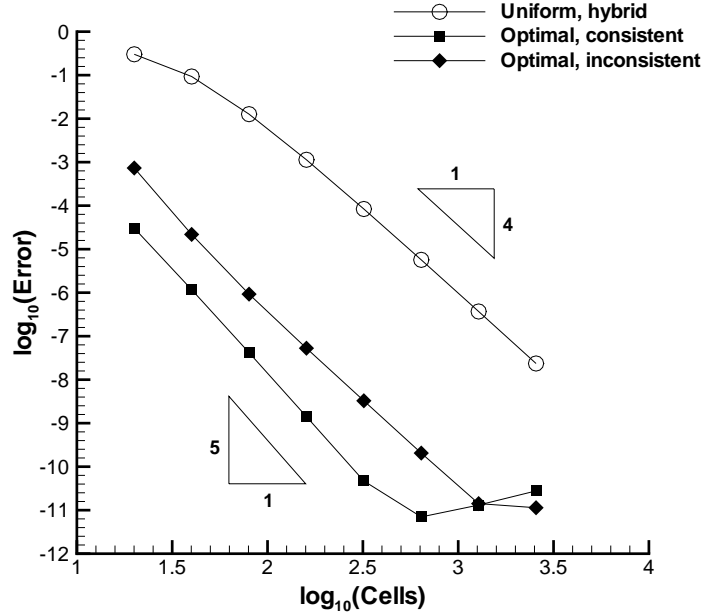


FIG. 4.13. Error convergence of a fourth-order hybrid approximation calculated with the consistent and inconsistent discretizations of the metric coefficient on the optimal and uniform grids.

The roots γ_2 and γ_3 are not appropriate because the second root does not meet the inequality Eq.(4.22) while the third root implies that $f(x) = x$. Therefore, the only non-trivial solution of Eq.(4.21), (4.22) is $\gamma + \theta = \alpha$. Introducing a parameter m so that $\gamma/\theta = m$ the particular solution of Eq.(3.6) can be written in the following form

$$(4.24) \quad \begin{aligned} x_{opt}(\xi, \eta) &= e^{\frac{-m\alpha}{m+1}\xi} e^{\eta} \\ y_{opt}(\xi, \eta) &= e^{\frac{-\alpha}{m+1}\xi} e^{\eta} \\ f(x, y) &= x^{-\frac{m+2}{m-1}} y^{\frac{2m+1}{m-1}}. \end{aligned}$$

In the present test example the parameters m and α have been chosen to be 10 and 3, respectively. The corresponding optimal 41×21 grid and 30 isolines of the function $f(x, y)$ are depicted in Fig.4.14. It is notable that the optimal grid is orthogonal neither in the domain nor at the boundaries. Moreover, the grid lines are concentrated near strong gradients and at the same time, they are not strictly aligned to the isolines of $f(x, y)$. A second-order accurate approximation of f_x is obtained by using two-point central differences for all the derivatives in Eq.(3.1). A uniform grid is generated by the transfinite interpolation of the boundary nodes, which are uniformly distributed along the boundaries. Since the optimal grid Eq.(4.24) has been constructed under the assumption that the leading term of the truncation error in the ξ coordinate vanishes on the optimal grid we shall refine the grid only in ξ while the number of grid cells in η is fixed and equal to 20. Note that the grid refinement in the η coordinate makes no influence on the convergence rate of the truncation error that is consistent with Eq.(3.6).

A comparison of the truncation error convergence obtained on the optimal and uniform grids is shown in Fig.4.15. Similarly to the 1D test examples, the global order of the symmetric second-order approximation in two dimensions is increased by more than one on the optimal grid. Furthermore, the L_2 norm of the truncation error is about 4 orders of magnitude less than that obtained on the corresponding uniform grid.

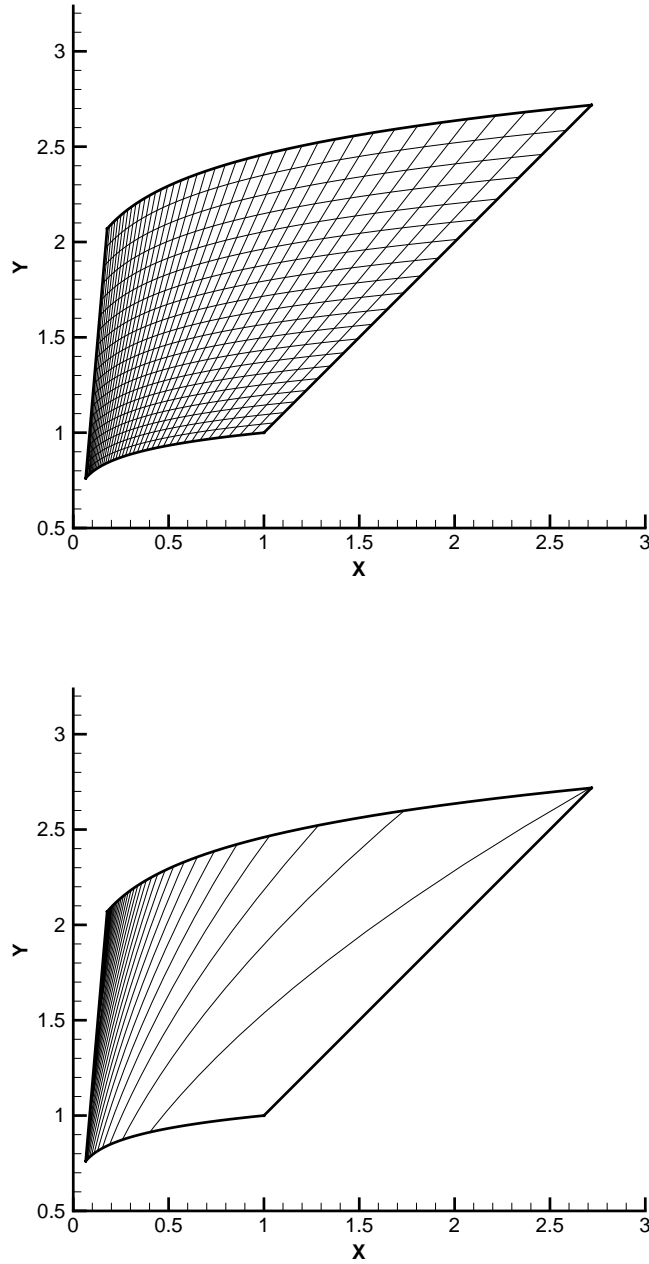


FIG. 4.14. *Optimal 40×20 grid and 30 isolines of the function $f(x)$.*

As can be seen in Fig.4.15, the new grid adaptation criterion enables one to reach the asymptotic convergence rate on coarse grids while the application of a third-order accurate discretization on the uniform grid does not permit us to get so essential reduction in the truncation error as on the optimal grid.

The importance of the identical approximation of the first derivatives f_ξ and f_η and the metric coefficients x_ξ , y_ξ , and x_η , y_η , respectively is illustrated in Fig.4.16. The figure shows that if f_ξ , x_ξ , and y_ξ are evaluated by the same hybrid discretization Eq.(4.3) the order of approximation in ξ is increased by one if grid points

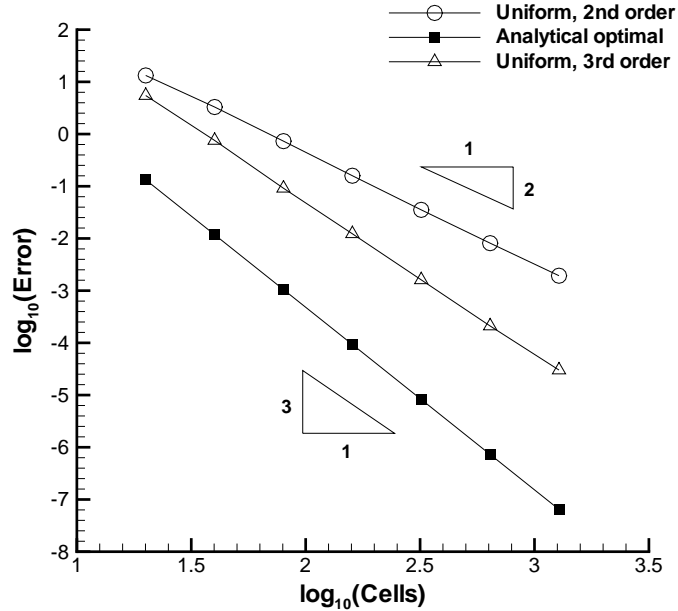


FIG. 4.15. Error convergence for a second-order approximation of f_x calculated on: 1) uniform grid, 2) analytical optimal grid, and 3) uniform grid using third-order accurate discretization.

are redistributed in accordance with Eq.(4.24) regardless what second-order approximations are used for f_η , x_η , and y_η . However, if the metric coefficients x_ξ and y_ξ are evaluated by the two-point symmetric second-order difference expression in the entire computational domain, whereas both the hybrid approximation of f_ξ Eq.(4.3) and the optimal grid Eq.(4.24) remain the same, the order of approximation of f_x in ξ deteriorates to 2 and the truncation error is increased by a factor of 10^3 .

5. Conclusion. The new grid adaptation strategy based on the minimization of the leading truncation error term of an arbitrary p th-order finite difference discretization has been developed. The basic idea of the method is to redistribute grid points so that the leading truncation error terms due to the differential operator and the metric coefficients cancel each other so that the design order of approximation on the optimal grid is increased by one in the entire computational domain. In contrast to most of the adaptive grid techniques, for the present method neither the truncation error estimate nor the specification of weighting parameters is required. Another very attractive characteristic of the new approach is its applicability to hybrid discretizations. It has been proved that if the differential operator and the metric coefficients are evaluated identically then the same optimal grid adaptation criterion, which is valid for non-hybrid discretizations, can be used in the entire computational domain regardless of points where the hybrid difference operator switches from one approximation to another. One of the main advantages of the new method is that it can be directly extended to multiple dimensions. It has been shown that the multidimensional grid adaptation criteria are fully consistent with the one-dimensional counterpart. The 1D and 2D numerical calculations show that the truncation error obtained on the optimal grid is both superconvergent and reduced by several orders of magnitude in comparison with the uniform and standard adaptive grid results for all the test examples considered.

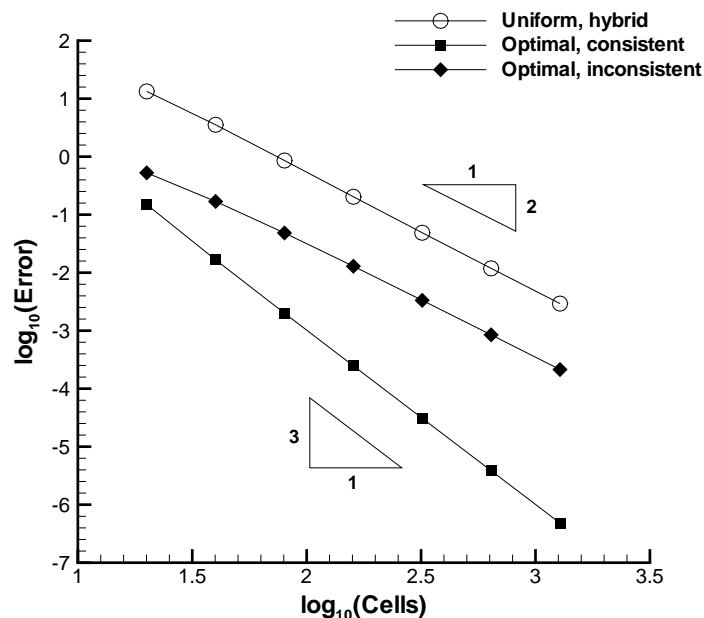


FIG. 4.16. Error convergence of a second-order hybrid approximation calculated with the consistent and inconsistent discretizations of the metric coefficient on the optimal and uniform grids.

Acknowledgments. The author would like to thank J.L. Thomas and M.H. Carpenter for many helpful discussions.

REFERENCES

- [1] J.F. THOMPSON AND C.W. MASTIN, *Order of difference expressions on curvilinear coordinate systems*, in Proc. ASME Fluid Engrg. Conf. Advances in Grid Generation, Houston, June 1983, p. 17.
- [2] J.D. HOFFMAN, *Relationship between the truncation errors of centered finite-difference approximation on uniform and nonuniform meshes*, J. Comput. Phys., **46** (1982), p. 469.
- [3] E. TURKEL, *Accuracy of schemes with nonuniform meshes for compressible fluid flows*, ICASE Report No. 85-43, (1985), p. 48.
- [4] I. BABUŠKA AND RHEINBOLDT, *A-posteriori error estimates for the finite element method*, Int. J. Numer. Methods Engrg., **12** (1978), p. 1597.
- [5] A.B. WHITE, *On selection of equidistributing meshes for two-point boundary-value problems*, SIAM J. Numer. Anal., **16**, No. 3 (1979), p. 472.
- [6] H.A. DWYER, *Grid adaptation for problems in fluid dynamics*, AIAA J., **22**, No. 12 (1984), p. 1705.
- [7] M. LETINI AND V. PEREYRA, *An adaptive finite difference solver for nonlinear two-point boundary problems with mild boundary layers*, SIAM J. Numer. Anal., **14**, No. 1 (1977), p. 91.
- [8] G.H. KLOPPER AND D.S. MCRAE, *The nonlinear modified equation approach to analyzing finite difference scheme*, AIAA Paper No. 81-1029, (1981), p. 317
- [9] V.E. DENNY AND R.B. LANDIS, *A new method for solving two-point boundary-value problems using optimal node distribution*, J. Comput. Phys., **9** (1972), p. 120.
- [10] B. PIERSON AND P. KUTLER, *Optimal nodal point distribution for improved accuracy in computational*

- fluid dynamics*, AIAA J., **18**, No. 1 (1980), p. 49.
- [11] D. VENDITTI AND D. DARMOFAL, *A multilevel error estimation and grid adaptive strategy for improving the accuracy of integral outputs*, AIAA Paper No. 99-3292, (1999).
- [12] G.F. CAREY AND H.T. DINH, *Grading functions and mesh redistribution*, SIAM J. Numer. Anal., **22**, No. 5 (1985), p. 1028.
- [13] K. CHEN, *Error equidistribution and mesh adaptation*, SIAM J. Sci. Comput., **15**, No. 4 (1994), p. 798.
- [14] W. RHEINBOLDT, *Adaptive mesh refinement processes for finite element solutions*, Int. J. Numer. Methods Engrg., **17** (1981), p. 649.
- [15] G.F. CAREY AND D. HUMPHREY, *Mesh refinement and iterative solution methods for finite element computations*, Int. J. Numer. Methods Engrg., **17** (1981), p. 1717.
- [16] A. MACKENZIE, D.F. MAYERS, AND A.J. MAYFIELD, *Error estimates and mesh adaptation for a cell vertex finite volume scheme*, Notes on Numerical Fluid Mechanics, **44** (1993), p. 291.
- [17] J.U. BRACKBILL AND J.S. SALTZMAN, *Adaptive zoning for singular problems in two dimensions*, J. of Comput. Phys., **46** (1982), p. 342.
- [18] J.F. THOMPSON, Z.U.A. WARSI, AND C.W. MASTIN, *Numerical Grid Generation: Foundation and Applications*, North Holland, p. 483, 1985.